

<sup>1</sup> **The offline luminosity measurement of data for studying XYZ  
2 particles at BESIII**

<sup>3</sup> Q. Gao, W. M. Song, J. Z. Zhang and C. Z. Yuan

**Abstract**

The XYZ particles discovered in recent years are of great interest as they may reveal the mysteries of chromodynamics (QCD) that is part of, unfortunately the poorest understanding part of, our current theory of everything, called the standard model. BESIII, a detector working at  $\tau$ -charm energy region, has a great potential both on precision measurement and on new discovery on these puzzling states. From May 2011 to June 2013, an unprecedented big data sample about  $3.4 \text{ fb}^{-1}$  at around 4 GeV has been collected to study the XYZ particles at the BESIII. This note is to describe the luminosity measurement of this data sample.

<sup>4</sup> PACS numbers:

5 **I. INTRODUCTION**

Luminosity is a key ingredient underlying the measurements of any physics processes, especially for the cross section measurement. In principle, any processes can be used to determine luminosity, however the QED processes are mostly used for their large production rates and simple final state topologies, and one more reason is their cross sections can be calculated in high precision. In this analysis, Bhabha process ( $e^+e^- \rightarrow (\gamma)e^+e^-$ ) is used to measure the luminosity and Digamma ( $e^+e^- \rightarrow \gamma\gamma$ ) process to do a cross check. The luminosity is calculated with

$$L = \frac{N^{obs}}{\sigma \times \epsilon},$$

6 where  $N^{obs}$  is the number of observed events from real data,  $\sigma$  is the cross section which  
7 is obtained from generator directly,  $\epsilon$  is the selection efficiency determined with exclusive  
8 Monte Carlo (MC) samples.

9 In order to estimate the systematic error caused by the tracking efficiency, two ways  
10 are used to select Bhabha events, Method I is using both the information from main drift  
11 chamber (MDC) and electromagnetic Calorimeter (EMC) (results of this method are taken  
12 as the final result), Method II is using the EMC information only.

13 **A. Some basic information about the QED generators**

14 To measure luminosity, event generators are necessary to calculate the cross section and  
15 to estimate the selection efficiency. So the understanding of the MC generators is an essen-  
16 tial part of luminosity measurement. Three MC generators frequently used in luminosity  
17 measurement are listed in Table I, which summarizes the methods of radiative corrections  
18 and theoretical accuracy for these generators. The Babayaga v3.5 is using QED Parton  
19 Shower approach for treatment of LL QED corrections; In Bhwide exact  $O(\alpha)$  correction-  
20 s are matches with the resummation of the infrared virtual and real photon contribution  
21 through the YFS exclusive exponentiation approach; The Babayaga@NLO is based on the  
22 matching of exact  $O(\alpha)$  correction with QED parton shower.

TABLE I: Monte Carlo generators for luminosity measurement.

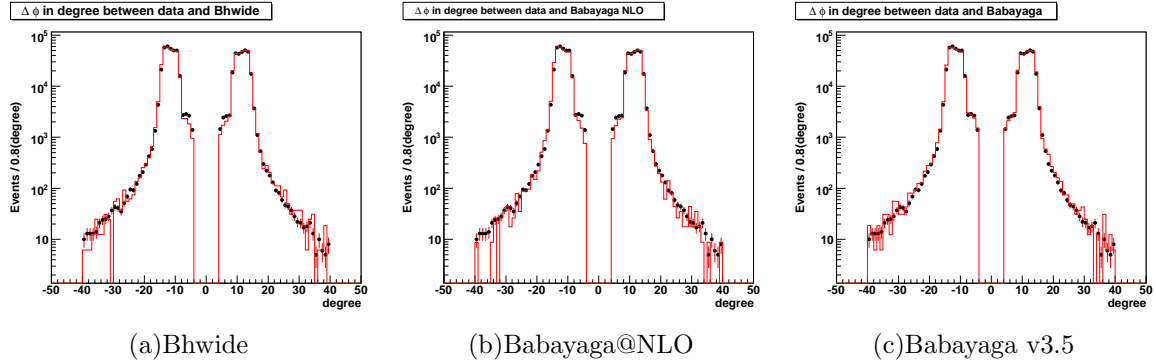
Generator	Theory	Accuracy at BESIII energy
Babayaga v3.5	Parton Shower	0.5%
Bhwide	$O(\alpha)$ + YFS	0.1%
Babayaga@NLO	$O(\alpha)$ PS	0.1%

23 In order to verify that these generators work well in the BESIII environment, the cross  
24 sections reported in Ref. [1] which was obtained by the authors of the generators and those  
25 calculated from the BESIII offline software system are compared. The results are shown in  
26 Table II, where the parameters for the generators are the same between the two compared  
27 sides.

28 From the comparison in Table II we can draw a conclusion that these generators work  
29 well at BESIII and can be used confidently.

TABLE II: Cross section comparison.

Generator	Cross Section in reference (nb)	Cross section at BESIII (nb)
Babayaga v3.5	6114.4	$6107.9 \pm 4.1$
Bhwid	6086.3	$6082.3 \pm 2.6$
Babayaga@NLO	6086.6	$6088.2 \pm 1.4$


 FIG. 1: The comparison of the  $\Delta\phi$  distribution between data and MC samples generated with three generators.

### 30 B. Choose the Monte Carlo generator

31 The uncertainty of the luminosity measurement is expected to be less than 1%, which is  
 32 dominant by generator used, so the generator chosen for efficiency measurement is of great  
 33 importance. Although, as shown in Table II, the cross sections from the three generators  
 34 are consistent with each other, the validity of them is not ensured as the angular and energy  
 35 distributions of the generated events are of importance too. The reason that we use the  
 36 Babayaga v3.5 instead of the other two is the later two can not simulate Bhabha events  
 37 with a energetic radiative photon well.

38 As seen in Fig. 1, events generated with Bhwid and Babayaga@NLO are not consistent  
 39 with the data well in the “shoulder” ( $|\Delta\phi| < 10^\circ$ , in which  $\Delta\phi = |\phi_{cluster1} - \phi_{cluster2}| -$   
 40  $180^\circ$ ) part, while Babayaga v3.5 can describe the data well. By checking the MC truth we  
 41 find that the events in the “shoulder” have such a large energy radiative photon that the  
 42 photon one with charged track are selected as the two most energetic clusters. As photon  
 43 does not bend in the magnetic field, the  $\Delta\phi$  peaks in half of that of two charged tracks.  
 44 From the comparisons of the ISR photon energy in Fig. 2, we can find that Bhwid and  
 45 Babayaga@NLO simulate less events with high energy ISR photon, so choose Babayaga v3.5  
 46 in this analysis.

47 And the option set in simulation for Bhabha events is shown in Table III. The option  
 48 for Di-gamma is the same as Bhabha except the Babayaga channel.

TABLE III: The option for MC simulation.

Option	Value	Comment
Channel	1	1 for Bhabha, 3 for Di-gamma.
Ebeam	2.13 GeV	Beam energy.
MinThetaAngle	20°	
MaxThetaAngle	160°	The range of polar angle is set a little larger than the detector.
MinimumEnergy	0.04 GeV	The minimum energy of particles produced.
MaximumAcollinearity	180°	The maximum acollinearity angle which is $180^\circ - \cos^{-1} \frac{\vec{P}_+ \cdot \vec{P}_-}{ \vec{P}_+  \vec{P}_- }$ .
RunningAlpha	1	With the $\alpha$ for QED running.
HadronicResonance	1	The hadronic resonance can be generated.
FSR swich	0	The final state radiation. It's only used in Di-mu process.
CUTG	0	Turn off ISR photon switch.
PHCUT	0	It's used for Di-gamma process to aviod double counting.

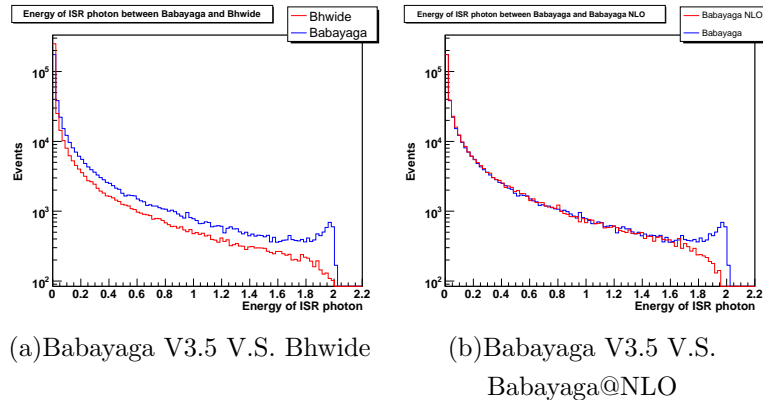


FIG. 2: The comparison of the energy distributions of ISR photon between MC truth samples from different MC generators.

### 49 C. The data samples to be measured

50 In Table IV, the information about the data samples is listed, including the requested  
 51 energy, the date of data taking, the RUN number and the online luminosity. The online  
 52 luminosity is estimated with Bhabha events recorded at the endcap of EMC during the  
 53 data taking. It is such a rough estimation that is only used for reference. The luminosity of  
 54 the data taken at 4009 MeV (No.1) has been measured using the same method, which can  
 55 be found in Ref.[3]. This memo is only about the data at the other 15 energy points.

## 56 II. EVENT SELECTION

### 57 A. The selection criteria of Bhabha events for nominal result in Method I

58 Two good charged tracks with each one originates from the interaction point with  $V_{xy} =$   
 59  $\sqrt{V_x^2 + V_y^2} < 1$  cm and  $|V_z| < 10$  cm are required, where  $V_x, V_y, V_z$  are the  $x, y, z$  coordinates

TABLE IV: A summary of the data samples.

No.	Energy (MeV)	Date (y-m-d)	RUN	Online lum. ( $\text{pb}^{-1}$ )
1	4009	2011-05-03 to 2011-06-01	23463-24141	470
2	4260 <sup>1</sup>	2012-12-14 to 2013-01-14	29677-30367	515
3	4190	2013-01-14 to 2013-01-16	30372-30437	42
4	4230 <sup>1</sup>	2013-01-16 to 2013-01-18	30438-30491	44
5	4310	2013-01-18 to 2013-01-20	30492-30557	44
6	4360	2013-01-26 to 2013-02-24	30616-31279	523
7	4390	2013-02-24 to 2013-02-26	31281-31325	53
8	4420	2013-02-26 to 2013-02-28	31327-31390	43
9	4260 <sup>2</sup>	2013-03-09 to 2013-03-22	31561-31981	289
10	4210	2013-03-22 to 2013-03-25	31983-32045	52
11	4220	2013-03-25 to 2013-03-29	32046-32140	52
12	4245	2013-03-29 to 2013-04-01	32141-32226	53
13	4230 <sup>2</sup>	2013-04-01 to 2013-05-25	32239-33484	1007
14	3810	2013-05-25 to 2013-05-29	33490-33556	48
15	3900	2013-05-29 to 2013-06-01	33572-33657	50
16	4090	2013-06-01 to 2013-06-03	33659-33719	49

60 of the point of closest approach to the run dependent interaction point respectively. Each  
 61 charged track should lie within the polar angle region  $|\cos\theta| < 0.8$ . And the net charge for  
 62 the two tracks should be zero. The deposited energies of electron and positron must both  
 63 be larger than  $\frac{1.55}{4.26} \times E_{\text{cms}}$  ( $E_{\text{cms}}$  is center-of-mass energy) to suppress Dimu background. And  
 64 the momenta of electron and positron are required to be larger than  $\frac{2}{4.26} \times E_{\text{cms}}$  to suppress  
 65 the backgrounds events from resonance such as  $J/\psi$  and  $\psi'$ . We summarize these selection  
 66 criteria as following, all the variables mentioned here are in the CMS frame.

- 67     • Two good charged tracks with net charge zero.  $V_{xy} < 1 \text{ cm}$ ,  $|V_z| < 10 \text{ cm}$  for each  
 68     track.  
 69     •  $E_{e^-}, E_{e^+} > \frac{1.55}{4.26} \times E_{\text{cms}}$ .  
 70     •  $|\cos\theta_{e^-}^{\text{MDC}}|, |\cos\theta_{e^+}^{\text{MDC}}| < 0.8$ .  
 71     •  $P_{e^-}, P_{e^+} > \frac{2}{4.26} \times E_{\text{cms}}$ .

72     **B. The selection criteria for Bhabha events in Method II and for Di-gamma events  
 73     as a cross check**

74     First, there should be at least two clusters in EMC. Since we don't use the information  
 75     of MDC, the background level is high, so we must tighten deposited energy criterion for  
 76     each cluster to  $\frac{1.8}{4.26} \times E_{\text{cms}}$ . The criterion for the angle is  $|\cos\theta_1^{\text{EMC}}|, |\cos\theta_2^{\text{EMC}}| < 0.8$  (1  
 77     and 2 mean the most energetic cluster and the second one). Because of the existence of the  
 78     magnetic field, tracks of electron and positron are not straight in MDC, so these two clusters  
 79     are not back-to-back in EMC. We require  $\Delta\phi$  in the range of  $[-40^\circ, -5^\circ]$  or  $[5^\circ, 40^\circ]$  to remove

80 the Di-gamma events together with a kind of “strange” cosmic rays (details can be found  
81 below). Here  $\Delta\phi = |\phi_1 - \phi_2| - 180^\circ$  (Fig. 33(e)).

82 For Di-gamma events, the selection criteria are almost the same as the above one. But  
83 photon is neutral and do not bend in magnetic field, so the two clusters from Di-gamma  
84 events are back-to-back. They are separated from the Bhabha process by requiring  $-0.8^\circ <$   
85  $\Delta\phi < 0.8^\circ$  (Fig. 47(e)).

86 We summarize these selection criteria as follow.

- 87 • At least two clusters in EMC, the two most energetic clusters are numbered 1 and 2.
- 88 •  $E_1, E_2 > \frac{1.8}{4.26} \times E_{\text{cms}}$ .
- 89 •  $|\cos\theta_1^{\text{EMC}}|, |\cos\theta_2^{\text{EMC}}| < 0.8$ .
- 90 • For Bhabha events  $\Delta\phi$  should be in the range of  $[-40^\circ, -5^\circ]$  or  $[5^\circ, 40^\circ]$ .
- 91 • For Di-gamma events  $\Delta\phi$  should be in the range of  $[-0.8^\circ, 0.8^\circ]$ .

### 92 C. The strange cosmic rays

93 Without the requirement on  $|\Delta\phi| < 40^\circ$ , we find many events which deposit a lot of  
94 energy in EMC, even larger than 5 GeV and these events distribute equally in the EMC, so  
95 they can not be from electron and positron collision or the hot channels of EMC.

96 By checking the distributions of  $\Delta\phi$  and  $\Delta\cos\theta$  of these events, we find that they are  
97 events with two clusters hit at almost a same position in EMC, as shown in Figure 3. And  
98 from the EVENTDISPLAY of these events, as shown in Fig. 4, we find these events are  
99 cosmic rays which crash the EMC and deposit a lot of energy in it and are reconstructed as  
100 two clusters.

101 We require that  $|\Delta\phi| < 40^\circ$  to reduce such events, as the  $\Delta\phi$  distribution of them peaks  
102 at  $-180^\circ$ , as shown in Fig. 3.

## 103 III. BACKGROUND LEVEL

104 After above selection, we estimate the background level with a  $500 \text{ pb}^{-1}$  inclusive MC  
105 sample generated at 4.26 GeV, the details of this MC samples can be found in Ref.[2], and  
106 compare it with the data taken at 4.26 GeV from RUN 31561 to RUN 31981, as shown in  
107 Tables V, VII, VIII. For method I, a kind of background is from the Di-gamma process  
108 and is only  $7/17852900 = 4 \times 10^{-7}$  of the signal in data. For method II, the dominant  
109 background is from the Di-gamma process and is only  $2716/21588898 = 0.01\%$  of the signal  
110 in data. For the Di-gamma process, the dominant background is from Bhabha process and  
111 is only  $4923/4118609 = 0.1\%$  of the signal in data.

112 The number of background events from ISR resonance in method I is small also, because  
113 the  $J/\psi$  peak is removed by momenta requirement.  $\psi'$  peak is also removed except two  
114 energy points, 3810 and 3900 MeV, but in which the possible maximum ratio of  $\psi'$  is very

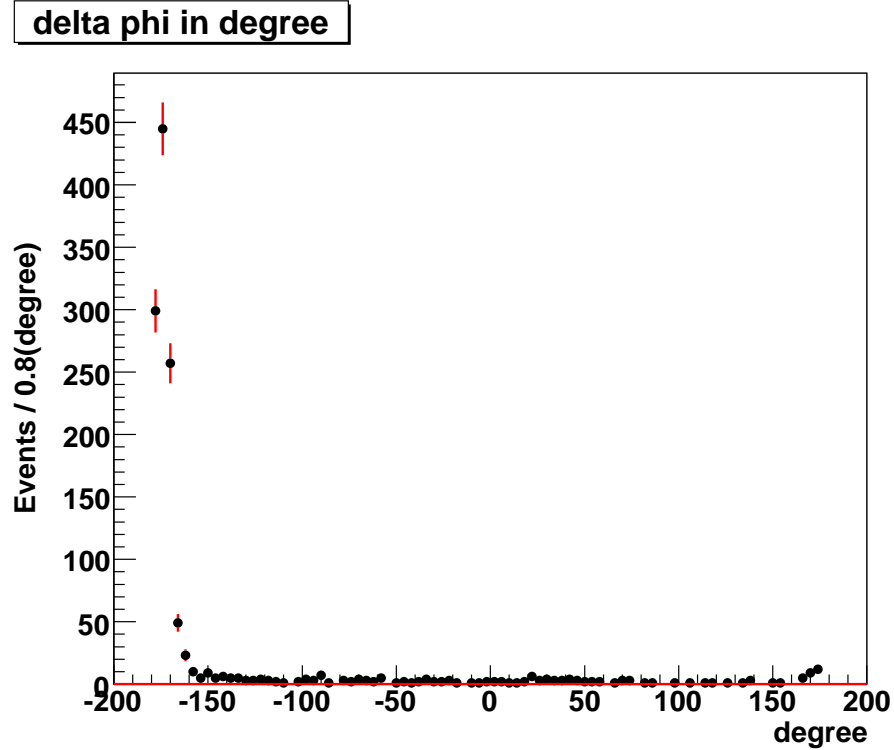


FIG. 3: The distribution of  $\Delta\phi$  for cosmic rays.

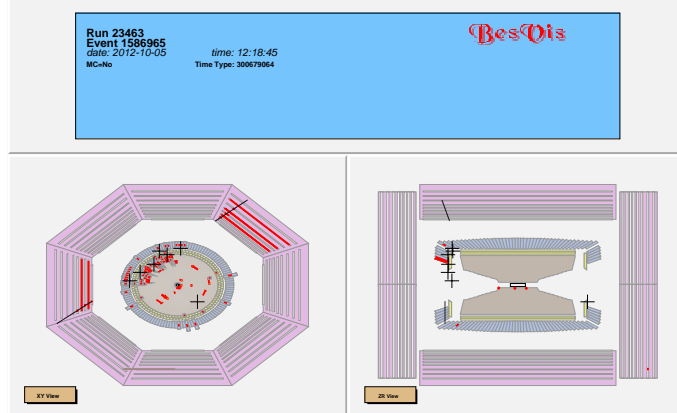


FIG. 4: The event display of a strange event.

115 low. For 3810 MeV, the online luminosity is  $48 \text{ pb}^{-1}$ , the cross section of  $\gamma_{ISR} \psi'$  is 2.0294  
 116 nb, the branching ratio of  $\psi' \rightarrow e^+e^-$  is  $7.73 \times 10^{-3}$ , so the number of  $e^+e^-$  from  $\psi'$  is  
 117  $48 \times 10^3 \times 2.0294 \times 7.73 \times 10^{-3} = 753$ . And the number of Bhabha events selected in method  
 118 I in the data is 3746950, so the maximum ratio of  $\psi'$  is  $753/3746950=2 \times 10^{-4}$ . And the  
 119 factor is  $1 \times 10^{-4}$  at 3900 MeV, which is shown in Table VI.

120 We conclude that the background level is so low that can be neglected.

TABLE V: Background level for Bhabha in method I.

Source	Number of events after selection
Bhabha from data	17852900
Dimu	3
Di-gamma	7
$q\bar{q}$	6
ISR	1
DD	1

TABLE VI: Background from  $\psi'$  peak for 3810 and 3900 MeV data in method I.

Energy(MeV)	$N_{Bhabha}$ in data	Luminosity online (pb $^{-1}$ )	$\sigma_{\gamma_{ISR}\psi'}(\text{nb})$	$B(\psi' \rightarrow e^+e^-)$	$N_{\psi'}$	Ratio
3810	3746950	48	2.0294	$7.73 \times 10^{-3}$	753	0.00020
3900	3727760	50	1.1634	$7.73 \times 10^{-3}$	450	0.00012

TABLE VII: Background level for Bhabha in method II.

Source	Number of events after selection
Signal from data	21588898
Dimu	1
Di-gamma	2716
$q\bar{q}$	13
ISR	117
$\gamma XYZ$	1
hadrons	21

TABLE VIII: Background level for Di-gamma process.

Source	Number of events after selection
Signal from data	4118609
Dimu	1
Bhabhaa	4923
$q\bar{q}$	7
ISR	2

## 121 IV. PRELIMINARY RESULT

122 We generate 1 million events at each energy point to calculate cross sections and efficiencies  
 123 for the Bhabha and the Di-gamma processes.

124 The numbers of events from data are shown in Table IX and Table X. The preliminary  
 125 results of the luminosity with statistical error are calculated with the formula in the intro-  
 126 duction part of this note, and are shown in Table XI, in which we find that the results from  
 127 Bhabha and Di-gamma process agree with each other well.

128 Meanwhile, we calculate the luminosity at 4260 MeV with other two generators, Bhwid-  
 129 e and Babayaga@NLO. The result is shown in Table XII. The results calculated by these

TABLE IX: The cross section of the Bhabha process, numbers of events ( $N_1$  and  $N_2$ ) and efficiencies ( $\epsilon_1$  and  $\epsilon_2$ ) for the two methods.

No.	Energy(MeV)	$\sigma_{Bhabha}$ (nb)	$N_1$	$\epsilon_1$ (%)	$N_2$	$\epsilon_2$ (%)
14	3810	508.08 $\pm$ 1.06	3746950	14.5924	4537102	17.8727
15	3900	485.82 $\pm$ 1.02	3727760	14.5849	4522186	17.8910
16	4090	440.86 $\pm$ 0.92	3373380	14.5391	4086378	17.7852
3	4190	421.03 $\pm$ 0.88	2638580	14.5442	3185817	17.7458
10	4210	417.60 $\pm$ 0.87	3308380	14.5239	3992965	17.7115
11	4220	415.62 $\pm$ 0.87	3276970	14.5647	3962824	17.7221
4	4230 <sup>1</sup>	413.50 $\pm$ 0.87	2663940	14.5080	3225569	17.6355
13	4230 <sup>2</sup>	413.50 $\pm$ 0.87	62766900	14.4933	76036612	17.6559
12	4245	410.62 $\pm$ 0.86	3311190	14.5067	4007053	17.6229
2	4260 <sup>1</sup>	407.75 $\pm$ 0.85	30884600	14.4620	37311288	17.6070
9	4260 <sup>2</sup>	407.75 $\pm$ 0.85	17852900	14.5012	21588898	17.6061
5	4310	398.29 $\pm$ 0.83	2590180	14.4825	3127020	17.5321
6	4360	389.34 $\pm$ 0.82	30430000	14.4780	36801586	17.5106
7	4390	384.20 $\pm$ 0.80	3062000	14.4421	3703999	17.4359
8	4420	379.38 $\pm$ 0.80	2453560	14.4764	2970473	17.3909

TABLE X: The cross section, number of events and efficiency for the Di-gamma process.

No.	Energy(MeV)	$\sigma_{Di-gamma}$ (nb)	$N_{Di-gamma}$	$\epsilon_{Di-gamma}$ (%)
14	3810	24.15 $\pm$ 0.04	497590	41.020
15	3900	23.05 $\pm$ 0.04	497380	41.061
16	4090	20.98 $\pm$ 0.04	450156	40.966
3	4190	19.99 $\pm$ 0.03	351618	40.830
10	4210	19.81 $\pm$ 0.03	437834	40.723
11	4220	19.71 $\pm$ 0.03	434670	40.675
4	4230 <sup>1</sup>	19.62 $\pm$ 0.03	356278	40.682
13	4230 <sup>2</sup>	19.62 $\pm$ 0.03	8313504	40.682
12	4245	19.49 $\pm$ 0.03	439092	40.576
2	4260 <sup>1</sup>	19.34 $\pm$ 0.03	4118609	40.597
9	4260 <sup>2</sup>	19.34 $\pm$ 0.03	2364167	40.597
5	4310	18.89 $\pm$ 0.03	346015	40.294
6	4360	18.46 $\pm$ 0.03	4030594	40.097
7	4390	18.22 $\pm$ 0.03	405944	39.867
8	4420	17.97 $\pm$ 0.03	324199	39.773

<sup>130</sup> three generators are consistent with each other, so the measurement is believable.

## <sup>131</sup> V. SYSTEMATIC ERROR

<sup>132</sup> A summary of the systematic errors is shown in Table XIV, including uncertainty from  
<sup>133</sup> the tracking efficiency, energy requirement, angle requirement, momentum requirement, the

TABLE XI: Preliminary results of the Bhabha and Di-gamma processes. The last two columns are results of method II and method I with the same selection criteria (named Method I(2)).

No.	Energy(MeV)	Method I( $\text{pb}^{-1}$ )	Di-gamma( $\text{pb}^{-1}$ )	Method II( $\text{pb}^{-1}$ )	Method I(2)( $\text{pb}^{-1}$ )
14	3810	50.54 $\pm$ 0.03	50.11 $\pm$ 0.08	49.96 $\pm$ 0.03	50.10 $\pm$ 0.03
15	3900	52.61 $\pm$ 0.03	52.57 $\pm$ 0.08	52.03 $\pm$ 0.03	52.11 $\pm$ 0.03
16	4090	52.63 $\pm$ 0.03	52.37 $\pm$ 0.08	52.12 $\pm$ 0.03	52.20 $\pm$ 0.03
3	4190	43.09 $\pm$ 0.03	43.08 $\pm$ 0.08	42.64 $\pm$ 0.03	42.80 $\pm$ 0.03
10	4210	54.55 $\pm$ 0.03	54.27 $\pm$ 0.09	53.98 $\pm$ 0.03	54.20 $\pm$ 0.04
11	4220	54.13 $\pm$ 0.03	54.22 $\pm$ 0.09	53.80 $\pm$ 0.03	53.86 $\pm$ 0.04
4	4230 <sup>1</sup>	44.40 $\pm$ 0.03	44.64 $\pm$ 0.08	44.23 $\pm$ 0.03	44.18 $\pm$ 0.03
13	4230 <sup>2</sup>	1047.34 $\pm$ 0.14	1041.56 $\pm$ 0.37	1041.50 $\pm$ 0.12	1041.72 $\pm$ 0.14
12	4245	55.59 $\pm$ 0.04	55.52 $\pm$ 0.09	55.37 $\pm$ 0.03	55.34 $\pm$ 0.04
2	4260 <sup>1</sup>	523.74 $\pm$ 0.10	524.57 $\pm$ 0.26	519.71 $\pm$ 0.09	521.26 $\pm$ 0.10
9	4260 <sup>2</sup>	301.93 $\pm$ 0.08	301.11 $\pm$ 0.20	300.73 $\pm$ 0.07	300.74 $\pm$ 0.08
5	4310	44.90 $\pm$ 0.03	45.46 $\pm$ 0.08	44.78 $\pm$ 0.03	44.82 $\pm$ 0.03
6	4360	539.84 $\pm$ 0.10	544.54 $\pm$ 0.28	539.80 $\pm$ 0.09	540.90 $\pm$ 0.10
7	4390	55.18 $\pm$ 0.04	55.89 $\pm$ 0.09	55.29 $\pm$ 0.03	55.39 $\pm$ 0.05
8	4420	44.67 $\pm$ 0.03	45.36 $\pm$ 0.08	45.02 $\pm$ 0.03	44.96 $\pm$ 0.03

TABLE XII: The luminosity at 4260 MeV is calculated by three generators.

No.	Energy(MeV)	Generator	Cross Section(nb)	Efficiency(%)	Number of Events	Lum. ( $\text{pb}^{-1}$ )
2	4260 <sup>1</sup>	Babayaga v3.5	407.75 $\pm$ 0.85	14.4620	30884600	523.74 $\pm$ 0.10
		Bhwid	402.07 $\pm$ 0.18	14.6971	30884600	522.65 $\pm$ 0.10
		Babayaga@NLO	400.75 $\pm$ 0.32	14.7482	30884600	522.55 $\pm$ 0.10
9	4260 <sup>2</sup>	Babayaga v3.5	407.75 $\pm$ 0.85	14.5012	17852900	301.93 $\pm$ 0.08
		Bhwid	402.07 $\pm$ 0.18	14.6971	17852900	302.12 $\pm$ 0.08
		Babayaga@NLO	400.75 $\pm$ 0.32	14.7482	17852900	302.06 $\pm$ 0.08

<sup>134</sup> statistics of the MC sample, total energy, and generator itself.

### <sup>135</sup> A. Tracking efficiency

<sup>136</sup> To estimate the systematic error due to the tracking. we compare the luminosity results  
<sup>137</sup> measured with or without using the MDC tracking information. To be fair, the selection  
<sup>138</sup> criteria about EMC information for method I must changed to be same with those of method  
<sup>139</sup> II, namely we require the deposited energies of electron and positron must both be larger than  
<sup>140</sup>  $\frac{1.8}{4.26} \times E_{\text{cms}}$ , and the  $\Delta\phi$  is in the range of  $[-40^\circ, -5^\circ]$  or  $[5^\circ, 40^\circ]$ , where  $\Delta\phi = |\phi_{e^-} - \phi_{e^+}| - 180^\circ$ .  
<sup>141</sup> We summarize the selection criteria of method I as follow.

- <sup>142</sup>
  - Two good charged tracks with net charge zero. For each track  $V_{xy} < 1 \text{ cm}$ ,  $|V_z| < 10 \text{ cm}$ .
  - $P_{e^-}, P_{e^+} > \frac{2}{4.26} \times E_{\text{cms}}$ .

- 145     •  $E_{e^-}, E_{e^+} > \frac{1.8}{4.26} \times E_{\text{cms}}$ .
- 146     •  $|\cos\theta_{e^-}^{\text{EMC}}|, |\cos\theta_{e^+}^{\text{EMC}}| < 0.8$ .
- 147     •  $\Delta\phi$  should be in the range of  $[-40^\circ, -5^\circ]$  or  $[5^\circ, 40^\circ]$ .

148     In method I, we use both MDC and EMC information, and in method II, we just use  
 149     EMC information, so the difference between these two methods is all about the tracking  
 150     efficiency. Taking 4260 MeV as an example, the measured luminosity of method I is 300.74  
 151      $\text{pb}^{-1}$  (Table XI) and that of method II is 300.73  $\text{pb}^{-1}$  (Table XI), so their difference is  
 152     0.004%. We take 0.004% as the systematic error for tracking efficiency for the data at 4260  
 153     MeV.

154     **B. Requirement on energy, angle and momentum**

155     Energies of electron and positron are required to be larger than 1.55 GeV at 4260 MeV.  
 156     We find that the energy distribution of MC is a little different from that of data (Fig. 19(a),  
 157     Fig. 19(b)), and choose a loose requirement. The systematic error is estimated by changing  
 158     1.55 GeV to 1.71 GeV (10% larger). The result is 301.82  $\text{pb}^{-1}$ , and it's 0.037% different  
 159     from the nominal result 301.93  $\text{pb}^{-1}$  (Table XI). We also try an other method of fit the data  
 160     with MC-determined shape convolved by a smearing function, and the smearing function is  
 161     a Crystal-ball, shown in Fig. 5(a), 5(b). The efficiency changes from 14.5135% to 14.5139%  
 162     (0.0028% in relative terms). 0.037% is much larger than 0.0028%, so we take 0.037% as  
 163     systematic error. For other energy points, we just use the first method to estimate the  
 164     systematic uncertainty caused by energy cut.

165     For angle cut, we require  $|\cos\theta|$  of electron and positron to be smaller than 0.8. We  
 166     estimate the systematic error caused by this by changing the requirement form 0.8 to 0.7.  
 167     For 4260 MeV, the luminosity changes from 301.93  $\text{pb}^{-1}$  (Table XI) to 302.33  $\text{pb}^{-1}$ . We take  
 168     their difference 0.14% as the systematic error for this item.

169     Momentum of electron and positron should be larger than 2 GeV at 4260 MeV in method  
 170     I. We find that the range of momentum distribution for MC is larger than that of data  
 171     (Fig. 19(e), Fig. 19(f)). We change 2 GeV to 2.06 GeV (3% larger) to get a new luminosity  
 172     result 301.73  $\text{pb}^{-1}$ . It's 0.068% different from the nominal result 301.93  $\text{pb}^{-1}$  (Table XI),  
 173     and this value is taken as the systematic error for the momentum requirement.

174     Similar to energy selection, we also try the method of fit. Because the momentum dis-  
 175     tribution of MC is wider than data, we fit the MC with the data shape convolved by a  
 176     smearing function, and the smearing function is a Gaussian, shown in Fig. 5(c), 5(d). In  
 177     this situation, the number of events of data will change instead of the efficiency when same  
 178     requirements are applied. The relative change on the luminosity result is 0.43%. We repeat  
 179     this procedure for some other energy points, such as 4090 MeV, 4230 MeV, 4360 MeV, and  
 180     we get the relative changes on luminosity results are 0.14%, 0.27%, 0.21%, respectively. And  
 181     the value of 0.43% at 4260 MeV is the largest one.

182     Figure 6 is an argument why we use the specific numbers above such as 10% larger, from  
 183     0.8 to 0.7 and 3% larger. For the energy requirement and momentum requirement, as shown  
 184     in Figures 7(a) and 7(b), the efficiency lost against these requirements is small, so we can

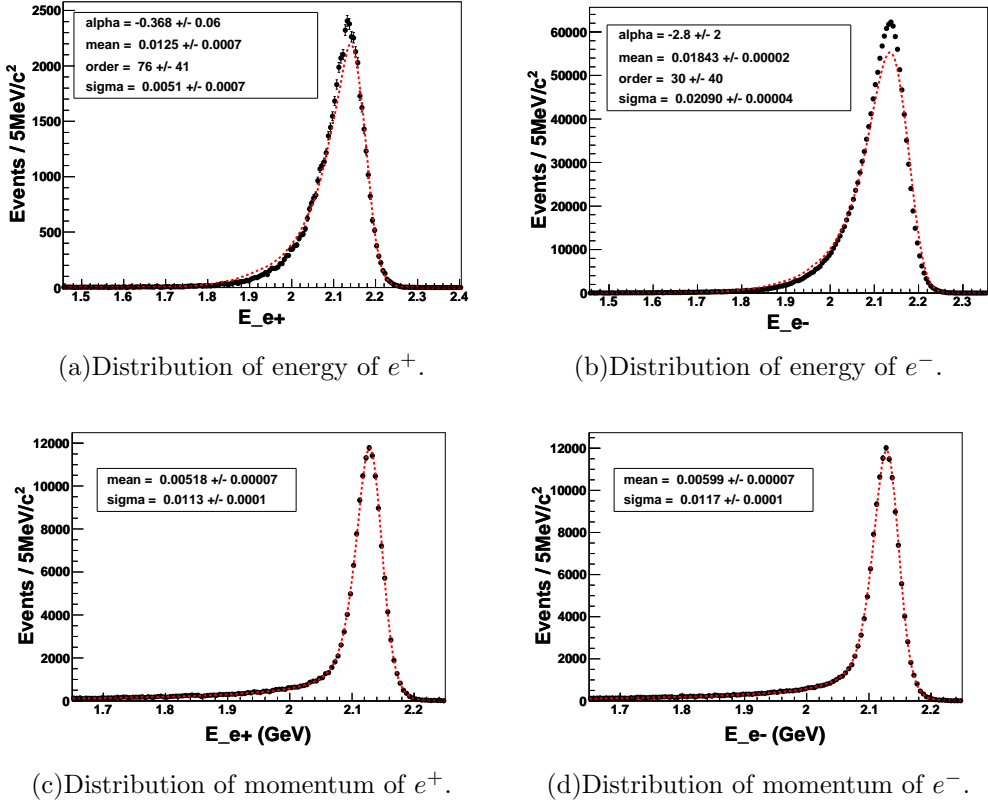


FIG. 5: Comparison of data and MC for energy and momentum distribution. Top two plots describe the data energy distribution fitted by MC shape convolved by a Crystal-ball function. Bottom two plots describe the MC momentum distribution fitted by the data shape convolved by a Gaussian function.

185 estimate the systematic errors caused by them by just changing requirements a little; as for  
 186 the  $\cos\theta$  requirement, we compare the numbers of events between data and MC in each bin,  
 187 as shown in Figures 7(c), and fit with a function  $p_0 \times (1 + p_1 * \cos^2\theta)$  to check the difference  
 188 data and MC. The  $p_1$  is very small means that the MC simulates the data well on the  $\cos\theta$   
 189 distribution, so the systematic error caused by this should not be large. We estimate it by  
 190 changing the requirement from  $|\cos\theta| < 0.8$  to  $|\cos\theta| < 0.7$ .

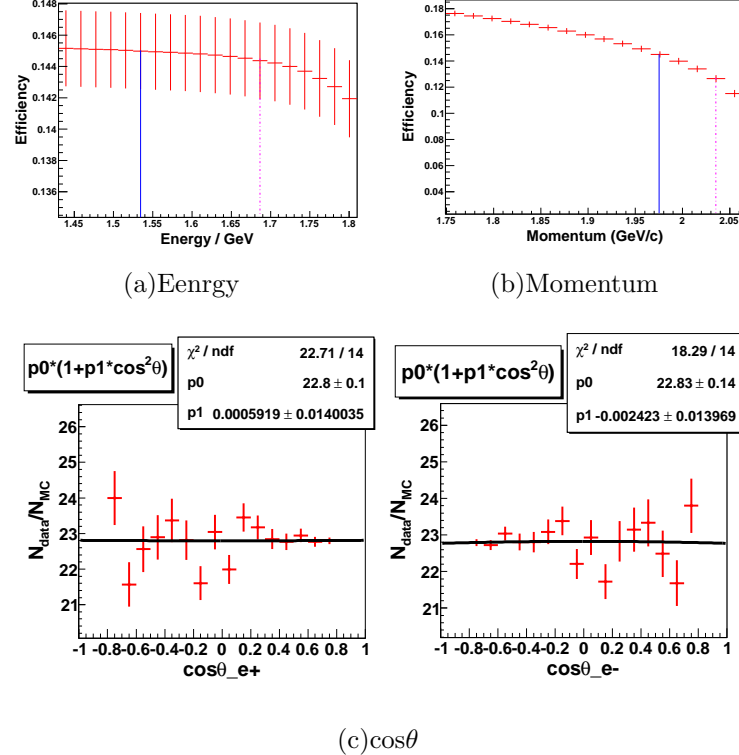


FIG. 6: The efficiency against the requirement on the energy (a), the momentum (b). The solid vertical lines tell the places where the requirements are made and the dash ones tell the changing. (c) is the ratio of events between data and MC in each bin of  $\cos\theta$ .

Figure 7 is to convince the reader that the estimation of the systematic error mentioned above is conservative by taking the measurement at 4210 MeV as an example. In the figure, the definition of the systematic error is  $\frac{\epsilon^{MC}}{\epsilon^{Data}} - 1$ , where the  $\epsilon = \frac{N}{N + \Delta N}$  (loosing the requirement) or  $\epsilon = \frac{N + \Delta N}{N}$  (tightening the requirement), here the  $\Delta N$  is the changing of the number of events when changing the requirement. The error of  $\frac{\epsilon^{MC}}{\epsilon^{Data}}$  is propagating from the errors of  $N^{Data}$ ,  $N^{MC}$ ,  $\Delta N^{Data}$  and  $\Delta N^{MC}$  by assuming there all follow Poisson distribution. From Figure 7, we conclude that the systematic error caused by these requirement should be small if any, and our estimation is conservative.

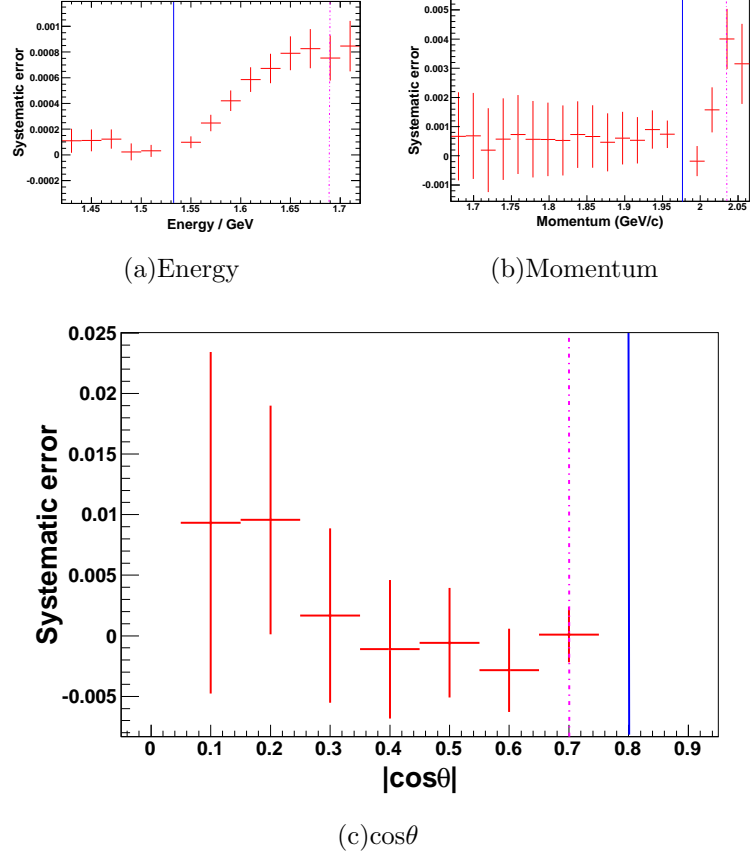


FIG. 7: The relative systematic errors for the requirements. The blue solid lines tell the nominal requirements applied in the analysis, the dash lines tell the changing ones used to estimate the systematic errors, the red crosses are the other changing values to verify the conservation of estimation.

199 We estimate the systematic error caused by tracking, the energy requirement, the angle  
 200 requirement and the momentum requirement for the data at the other energy points by the  
 201 same method as mentioned above, as shown in Table XIII. We use two methods to get a  
 202 nominal value among these points, one is to average them naively, the other is to pick up  
 203 the maximum one, as shown in Fig. 8. For momentum requirement, we take the maximum  
 204 uncertainty as 0.43% instead of 0.37%.

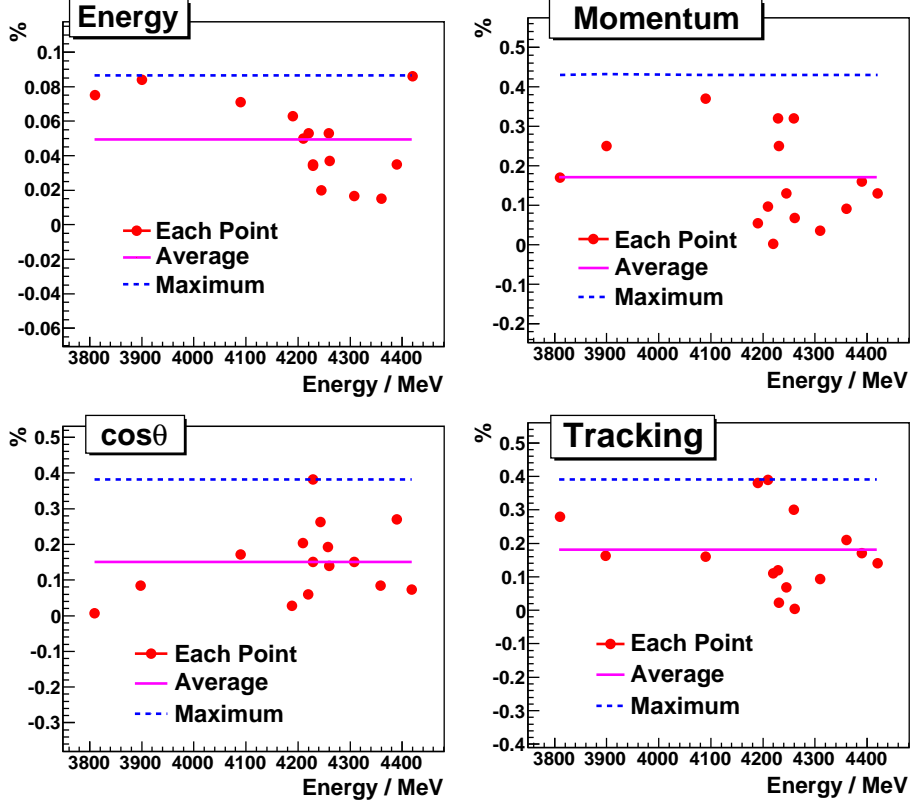


FIG. 8: The systematic errors caused by some requirements and tracking efficiency.

205 **C. Others**

206 We get the efficiencies with 1 M Bhabha events, and the statistical error of which is  
 207  $\sqrt{\frac{(1-\epsilon)}{\epsilon \times 1000000}}$ . For 4260 MeV, the efficiency is 14.5012% (Table IX), so the statistical error is  
 208 0.25% and it is taken as systematic error for efficiency.

209 We get the  $E_{\text{cms}}$  from beam energy measurement system (BEMS) which measures energy  
 210 using Compton back scattering technique, and the beam energy we get from BEMS has a  
 211  $\pm 1$  MeV uncertainty. For  $\text{sqrt}s = 4230$  MeV data, we generate another 1 M new MC sample  
 212 at 4232 MeV, the cross section is  $413.43 \pm 0.87$  nb and the selection efficiency is 14.5559%.  
 213 With this efficiency and cross section, we get the final luminosity  $1043.01 \text{ pb}^{-1}$ . Comparing  
 214 with the nominal result of  $1047.34 \text{ pb}^{-1}$ , the difference is 0.42%. For  $\sqrt{s} = 4260$  MeV data,  
 215 we generate another 1 M new MC sample at 4262 MeV, the luminosity of data with this  
 216 sample is  $301.00 \text{ pb}^{-1}$ , which is 0.31% different from the nominal result  $301.93 \text{ pb}^{-1}$ . We  
 217 also simulate a new MC sample of 1 M events at 4358 MeV, which is 2 MeV lower than  
 218 4360 MeV. The luminosity calculated with the MC-determined efficiency and cross section  
 219 at 4358 MeV is  $538.42 \pm 0.10 \text{ pb}^{-1}$  and difference between this value and the nominal one  
 220  $539.84 \pm 0.10 \text{ pb}^{-1}$  is 0.27%. We take the largest one 0.42% as the systematic error for all  
 221 the energy points. We can see that this is related to efficiency and cross section, so they

TABLE XIII: The resulting luminosity by changing the requirements: the third column is energy requirement changing from  $\frac{1.55}{4.26} \times E_{\text{cms}}$  to  $\frac{1.71}{4.26} \times E_{\text{cms}}$ ; the forth column is  $|\cos\theta|$  requirement changing from 0.8 to 0.7; the fifth column is momentum requirement changing from  $\frac{2}{4.26} \times E_{\text{cms}}$  to  $\frac{2.06}{4.26} \times E_{\text{cms}}$ .

No.	Energy(MeV)	Change Cut <sub>E</sub> (pb <sup>-1</sup> )	Change Cut <sub><math>\cos\theta</math></sub> (pb <sup>-1</sup> )	Change Cut <sub>P</sub> (pb <sup>-1</sup> )
14	3810	50.50±0.03	50.54±0.04	50.45±0.03
15	3900	52.57±0.03	52.65±0.04	52.48±0.03
16	4090	52.59±0.03	52.72±0.04	52.44±0.04
3	4190	43.06±0.03	43.10±0.04	43.07±0.03
10	4210	54.52±0.04	54.65±0.04	54.49±0.04
11	4220	54.11±0.03	54.16±0.04	54.13±0.04
4	4230 <sup>1</sup>	44.39±0.03	44.57±0.04	44.26±0.03
13	4230 <sup>2</sup>	1046.99±0.14	1048.87±0.18	1044.81±0.15
12	4245	55.58±0.04	55.73±0.05	55.52±0.04
2	4260 <sup>1</sup>	523.47±0.10	524.72±0.13	522.07±0.11
9	4260 <sup>2</sup>	301.82±0.08	302.33±0.10	301.73±0.08
5	4310	44.90±0.03	44.97±0.04	44.89±0.03
6	4360	539.92±0.10	540.28±0.13	539.35±0.11
7	4390	55.20±0.04	55.33±0.05	55.10±0.04
8	4420	44.71±0.03	44.71±0.04	44.62±0.04

222 are not independent with each other, but we consider them independent for conservative  
223 estimation.

224 The trigger efficiency for barrel Bhabha events approaches 100% for  $J/\psi$  and  $\psi'$  data  
225 taken in 2009 with an error less than 0.1% [4]. The trigger table of these data samples are  
226 the same as those used in  $J/\psi$  and  $\psi'$  data taking, and the most relevant trigger thresholds  
227 for Bhabha events are the EMC energy thresholds which should be more efficient for XYZ  
228 data since the center of mass energies are higher than in  $J/\psi$  and  $\psi'$  case. We take 0.1% as  
229 the systematic error caused by this.

230 The uncertainty of generator Babayaga v3.5 is 0.5%[1].

231 The summary of the systematic errors can be found in Table XIV and Fig. 9, from which  
232 we conclude that no matter which method (the averaged one or the maximum one) is picked  
233 to calculated the total systematic error, the result is less than 1%, so we recommend the  
234 value 1% to be used in the other physics analysis works if not sensitive to such a tiny  
235 difference.

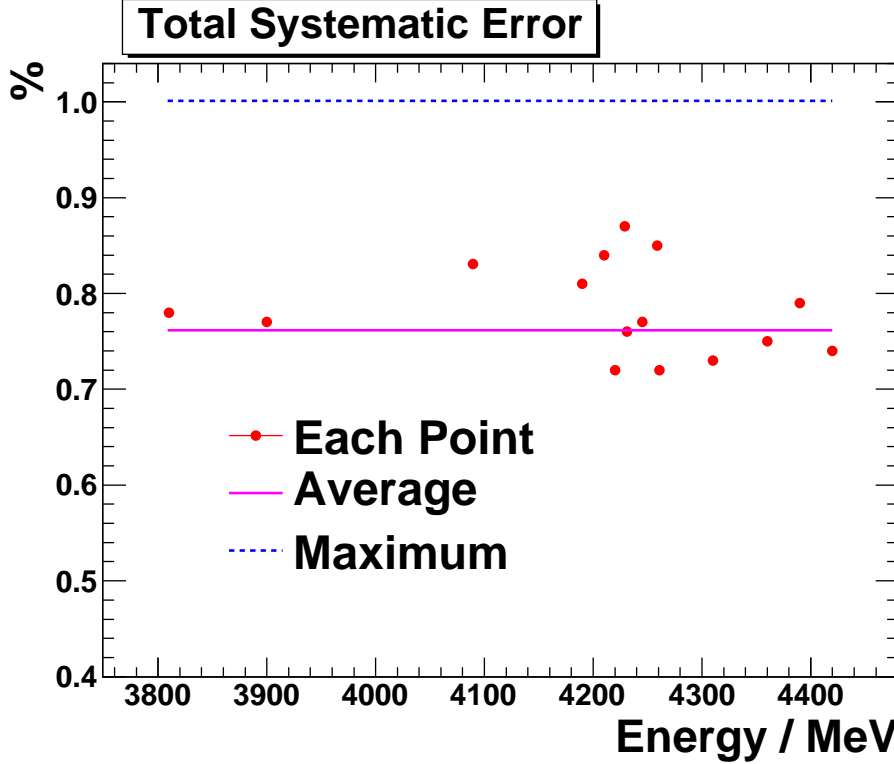


FIG. 9: The total systematic error.

TABLE XIV: A summary of systematic errors (%). The maximum uncertainty for  $\text{Cut}_P$  is taken as 0.43% with the method of fitting MC with data shape convolved by a smearing Gaussian function.

No.	Energy(MeV)	Tracking	$\text{Cut}_E$	$\text{Cut}_{\cos\theta}$	$\text{Cut}_P$	MC statistic	Energy-bias	Trigger efficiency	Generator	Total
14	3810	0.28	0.075	0.0046	0.17	0.25	0.42	0.10	0.50	0.79
15	3900	0.16	0.084	0.081	0.25	0.25	0.42	0.10	0.50	0.78
16	4090	0.16	0.071	0.17	0.37	0.25	0.42	0.10	0.50	0.84
3	4190	0.38	0.063	0.025	0.054	0.25	0.42	0.10	0.50	0.81
10	4210	0.39	0.050	0.20	0.096	0.25	0.42	0.10	0.50	0.84
11	4220	0.11	0.053	0.056	5.6E-4	0.25	0.42	0.10	0.50	0.72
4	4230 <sup>1</sup>	0.12	0.035	0.38	0.32	0.25	0.42	0.10	0.50	0.88
13	4230 <sup>2</sup>	0.022	0.036	0.15	0.25	0.25	0.42	0.10	0.50	0.77
12	4245	0.068	0.020	0.26	0.13	0.25	0.42	0.10	0.50	0.77
2	4260 <sup>1</sup>	0.30	0.053	0.19	0.32	0.25	0.42	0.10	0.50	0.86
9	4260 <sup>2</sup>	0.004	0.037	0.14	0.068	0.25	0.42	0.10	0.50	0.73
5	4310	0.093	0.016	0.15	0.035	0.25	0.42	0.10	0.50	0.73
6	4360	0.21	0.015	0.082	0.091	0.25	0.42	0.10	0.50	0.75
7	4390	0.17	0.035	0.27	0.16	0.25	0.42	0.10	0.50	0.80
8	4420	0.14	0.086	0.073	0.13	0.25	0.42	0.10	0.50	0.74
Average		0.18	0.049	0.15	0.17	0.25	0.42	0.10	0.50	0.77
Maximum		0.39	0.086	0.38	0.43	0.25	0.42	0.10	0.50	1.00

## 236 VI. THE COMPARISON BETWEEN DATA AND MC SIMULATION

237 The comparisons between data and MC simulation in method I, method II and Di-gamma  
 238 processes are shown in following plots, where we can find that the MC fits the data well.  
 239 When drawing these plots, only a fraction of data is used, and the data is normalized to  
 240 MC.

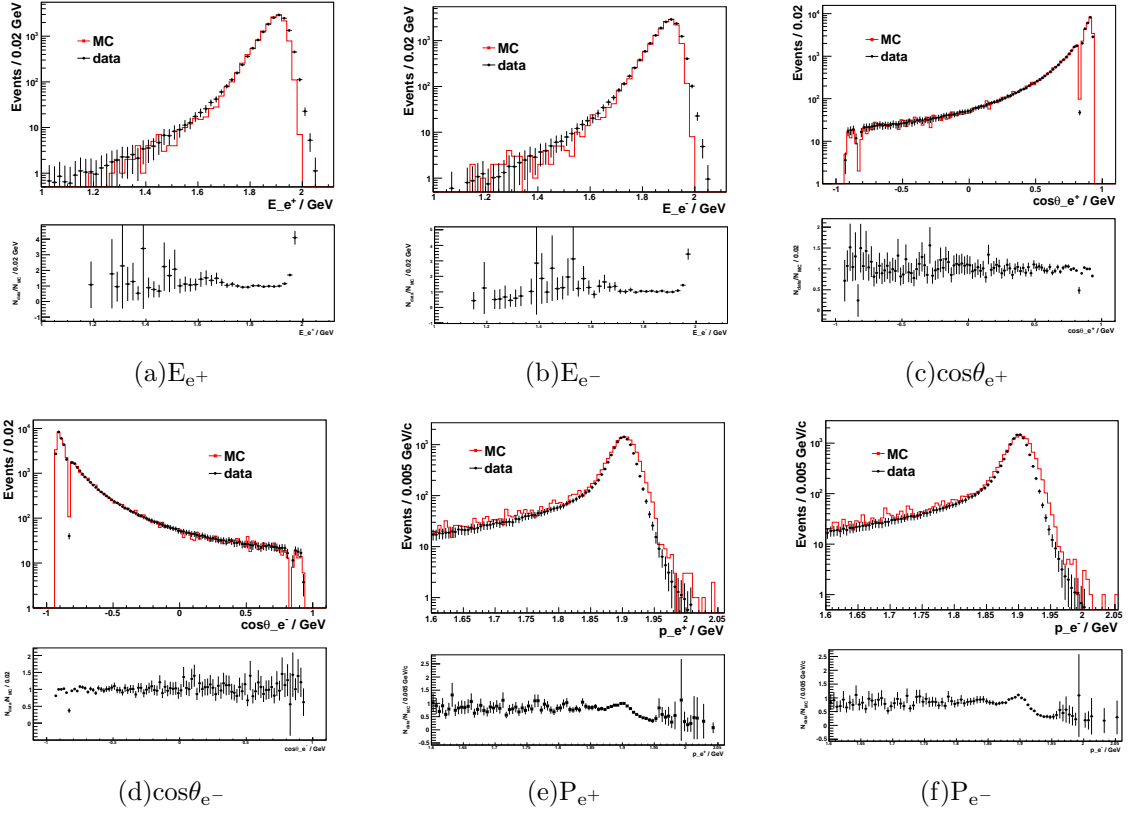


FIG. 10: The comparisons between data and MC in method I at 3810 MeV.

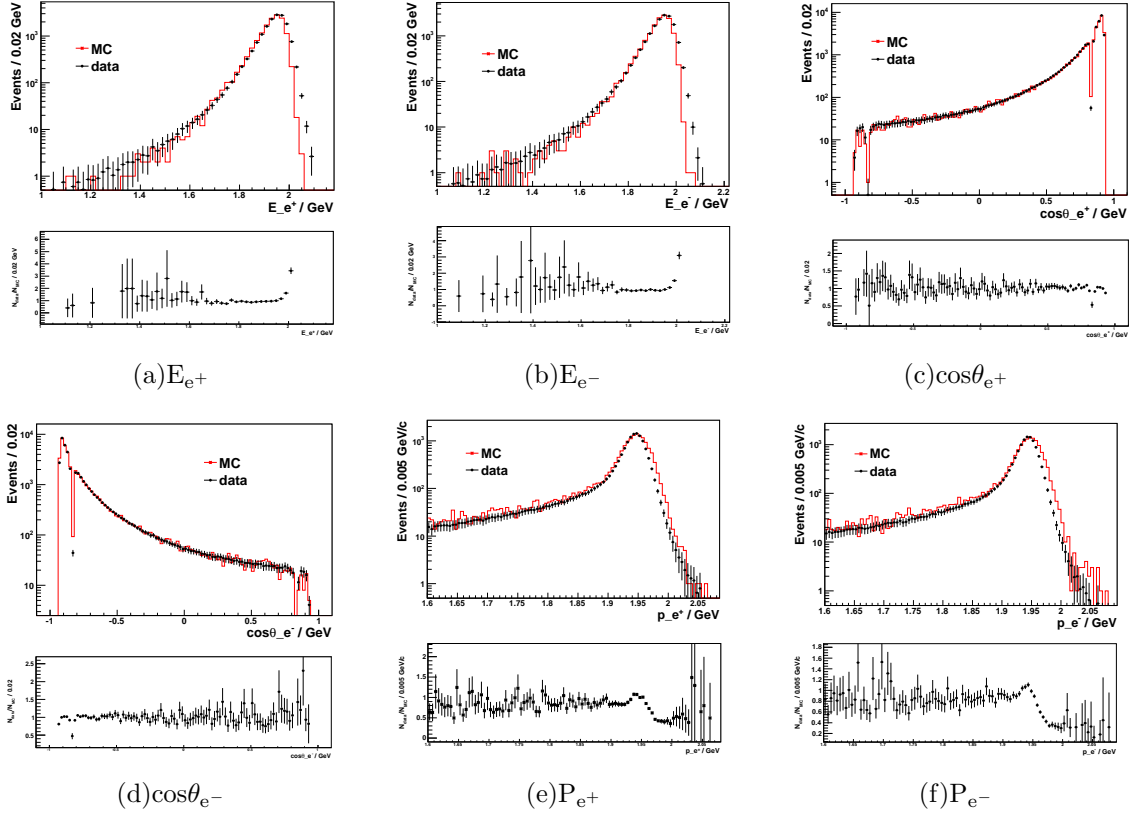


FIG. 11: The comparisons between data and MC in method I at 3900 MeV.

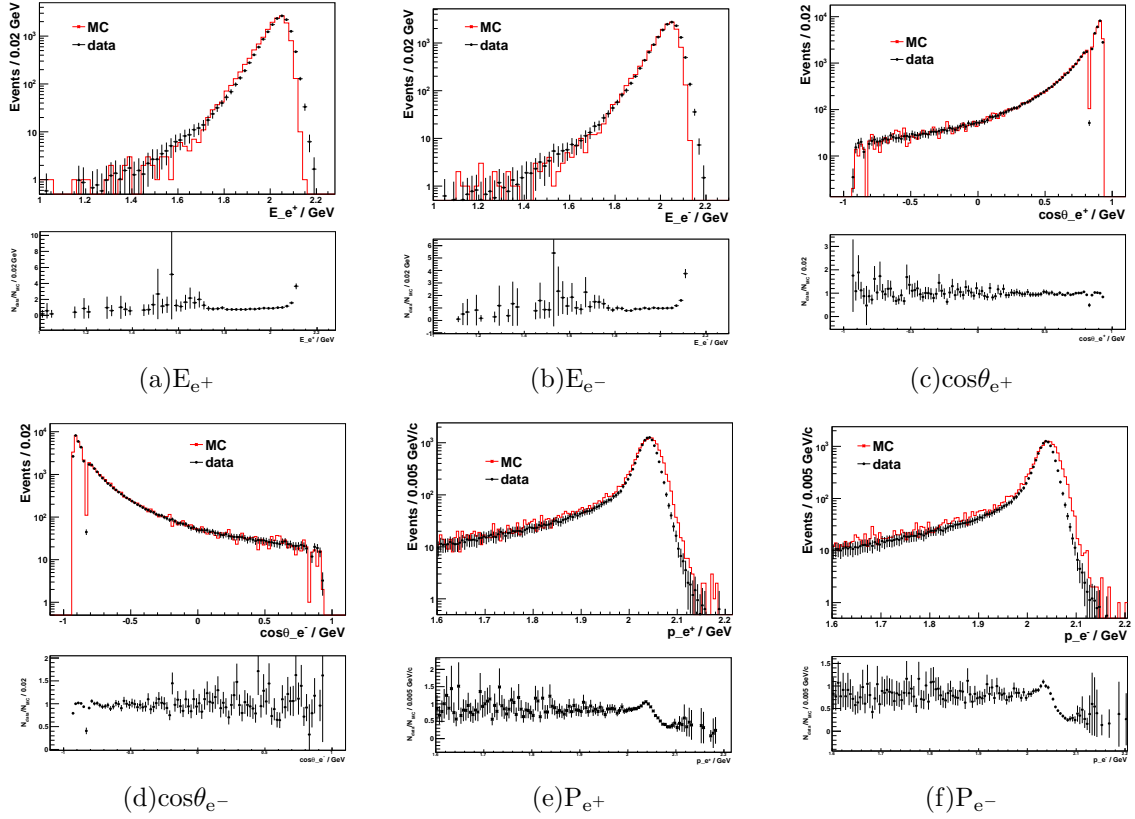


FIG. 12: The comparisons between data and MC in method I at 4090 MeV.

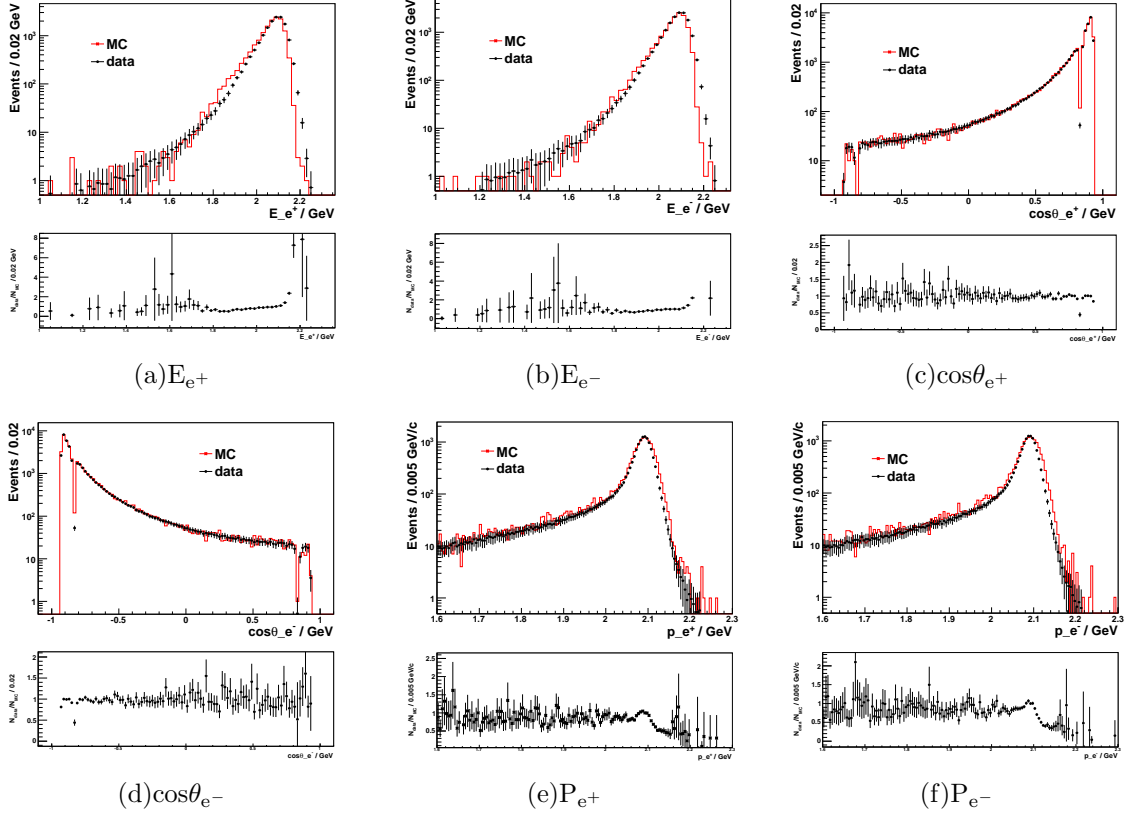


FIG. 13: The comparisons between data and MC in method I at 4190 MeV.

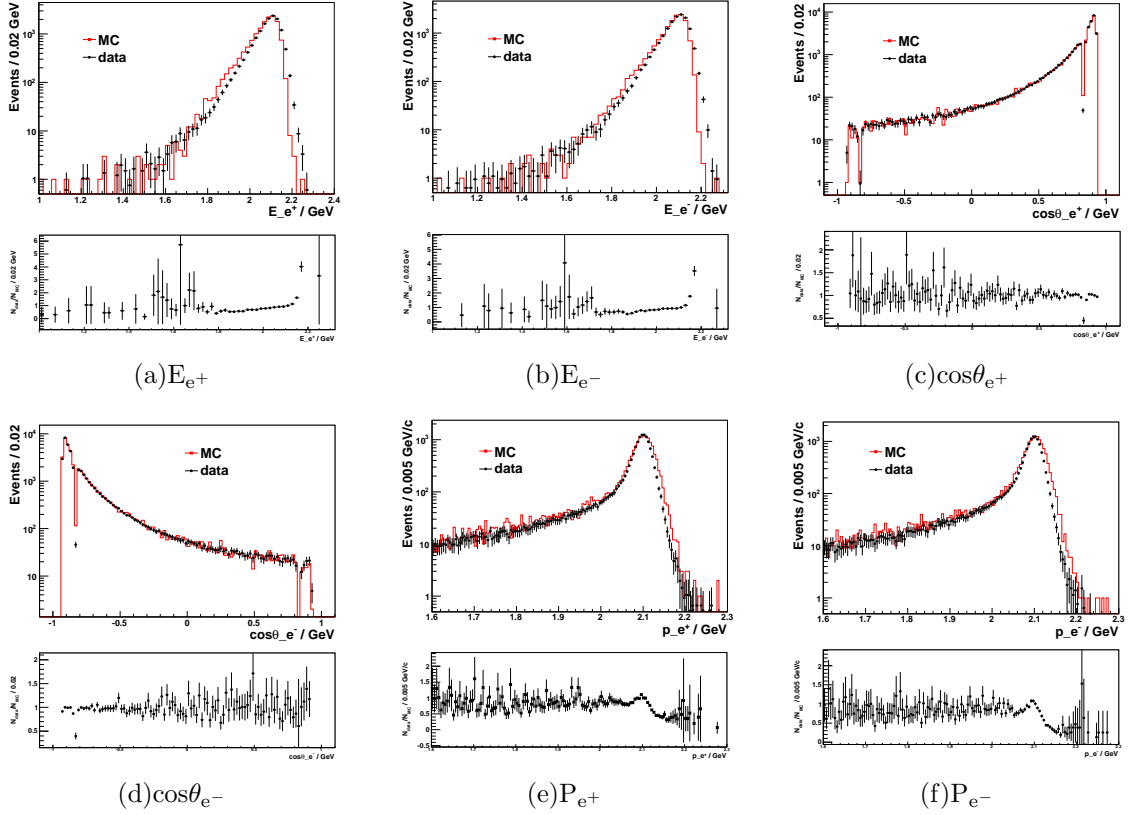


FIG. 14: The comparisons between data and MC in method I at 4210 MeV.

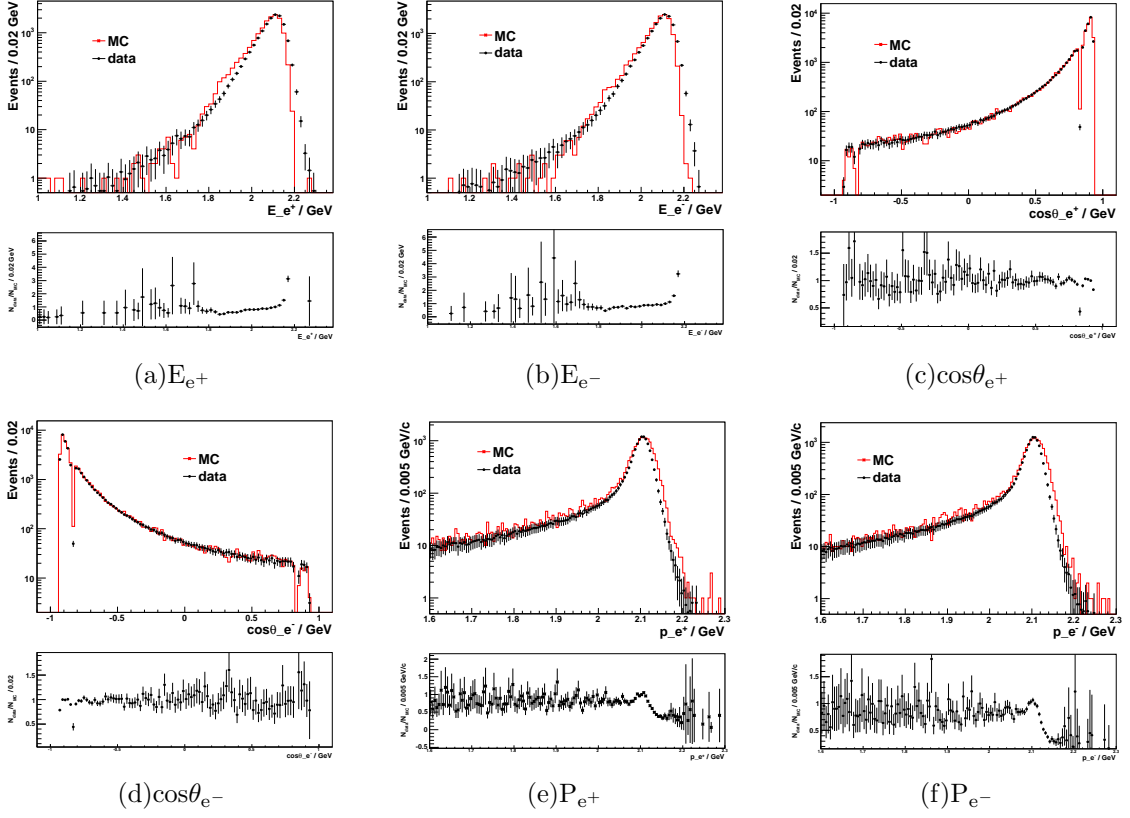


FIG. 15: The comparisons between data and MC in method I at 4220 MeV.

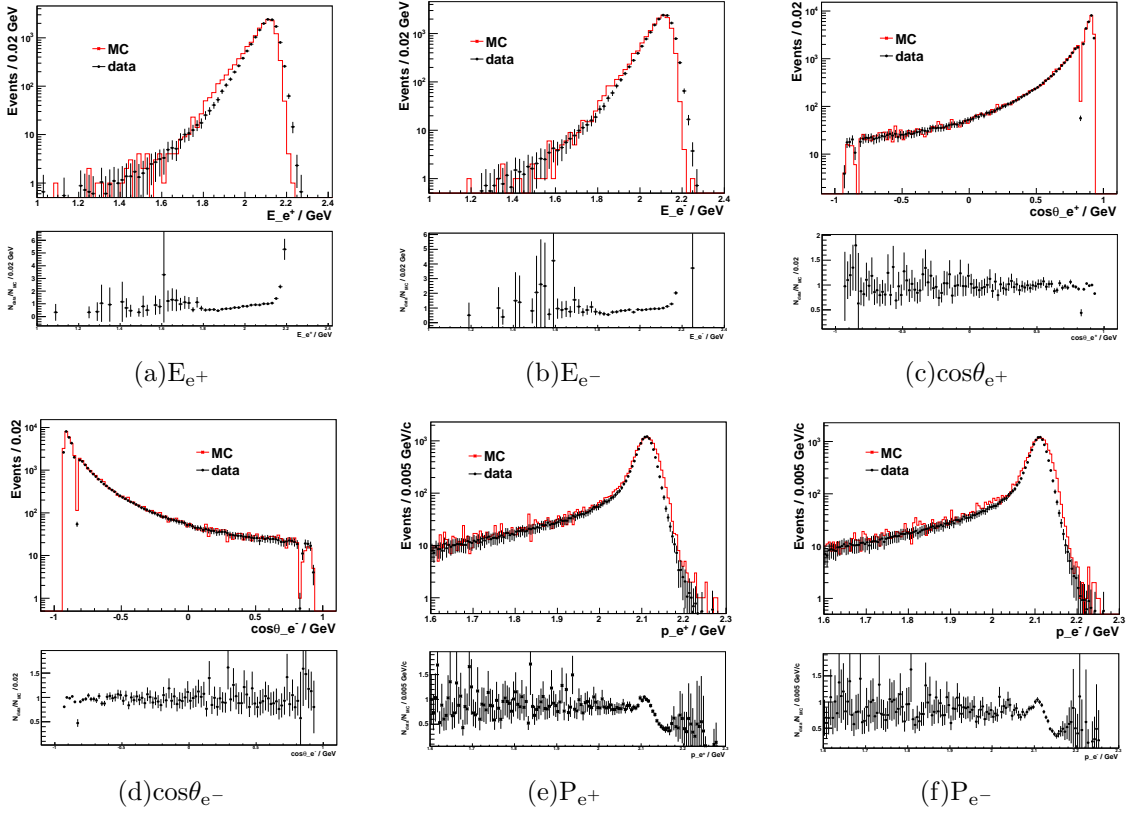


FIG. 16: The comparisons between data and MC in method I at  $4230^1$  MeV.

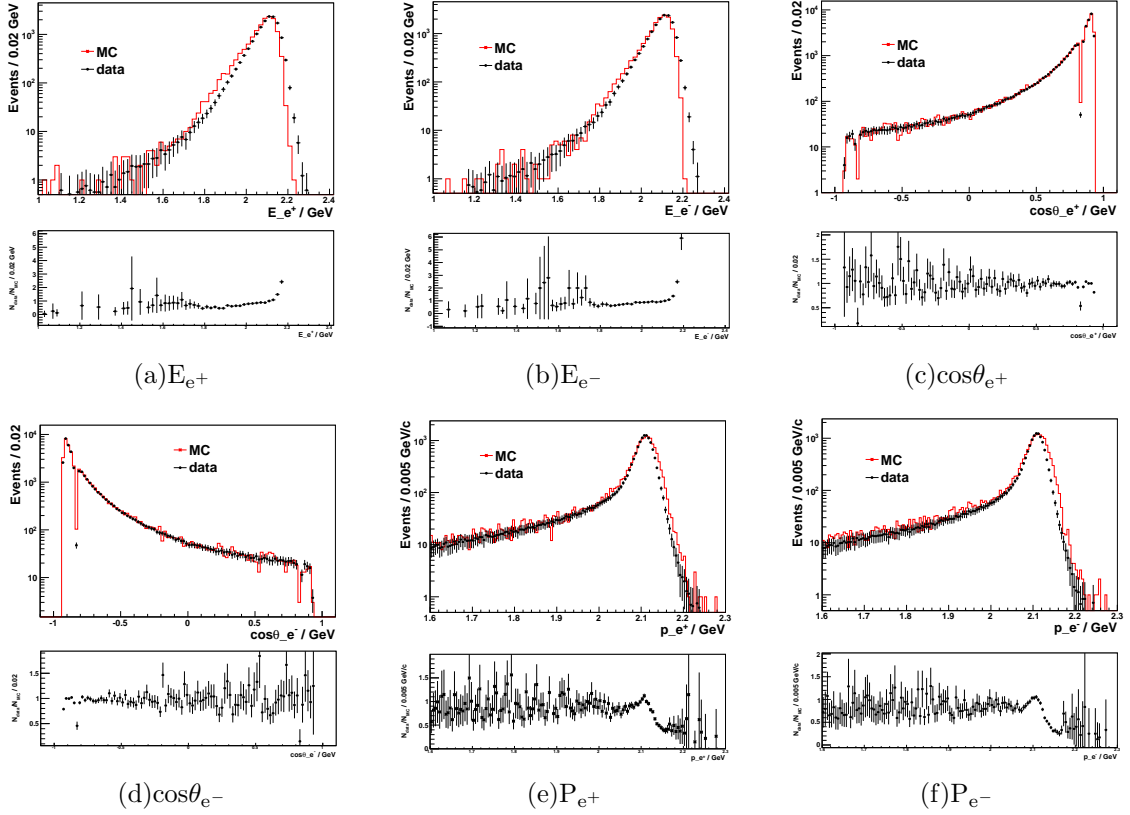


FIG. 17: The comparisons between data and MC in method I at  $4230^2$  MeV.

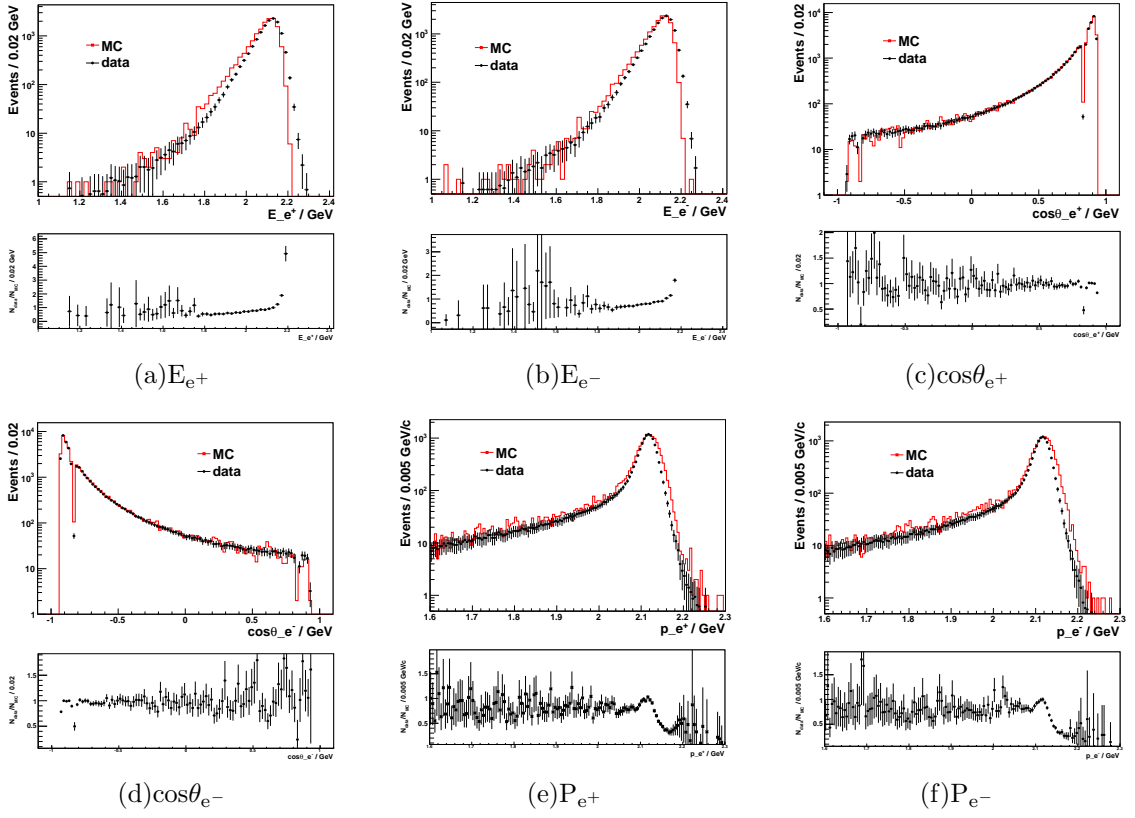


FIG. 18: The comparisons between data and MC in method I at 4245 MeV.

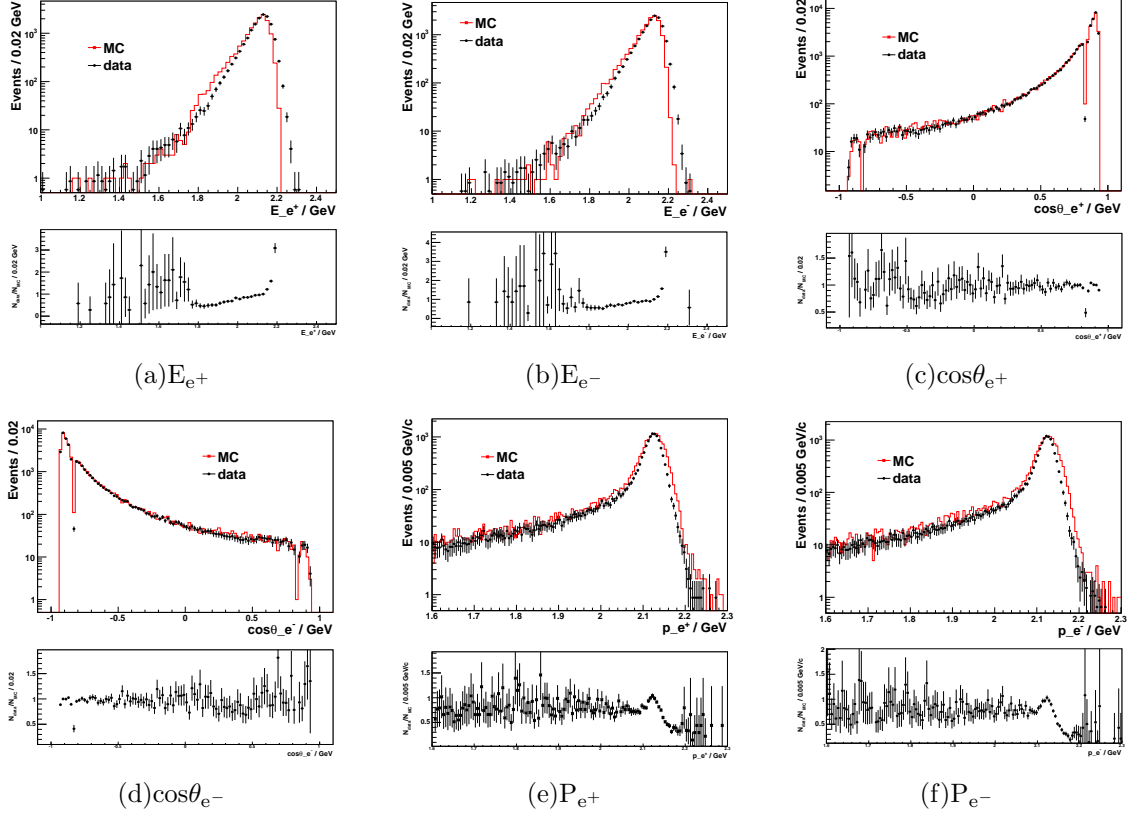


FIG. 19: The comparisons between data and MC in method I at 4260 MeV.

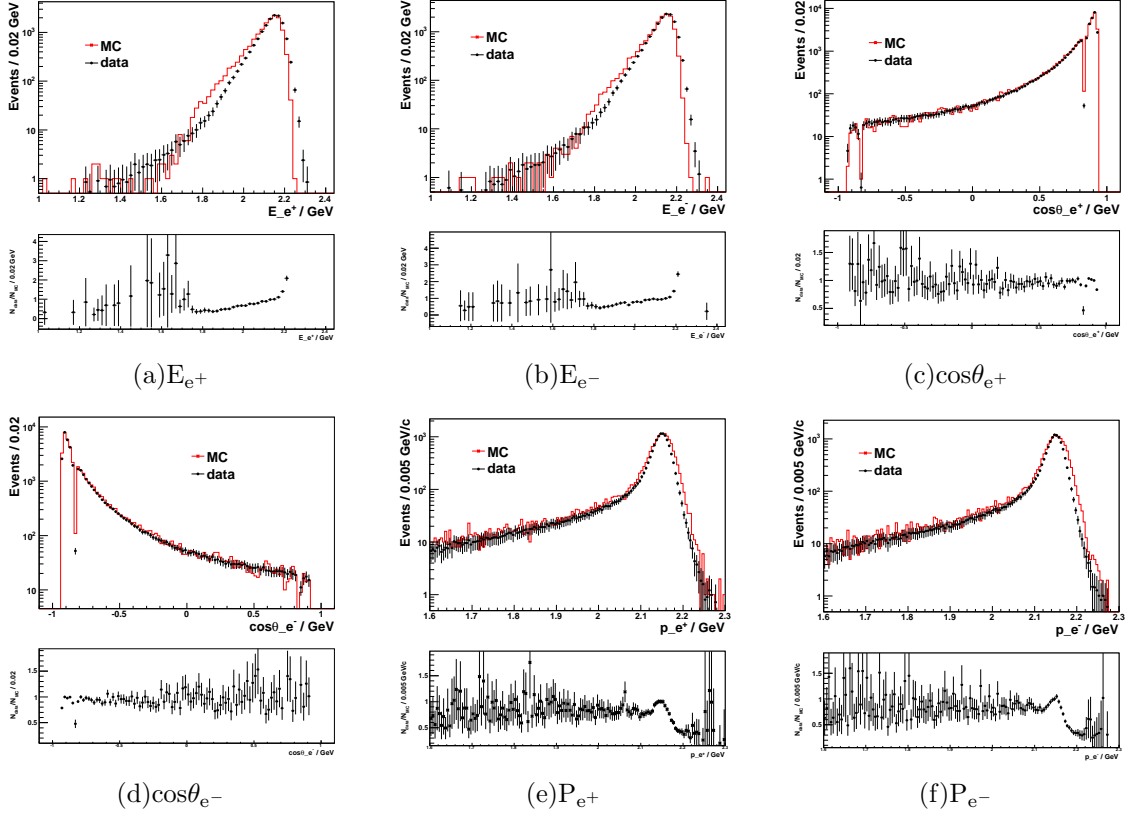


FIG. 20: The comparisons between data and MC in method I at 4310 MeV.

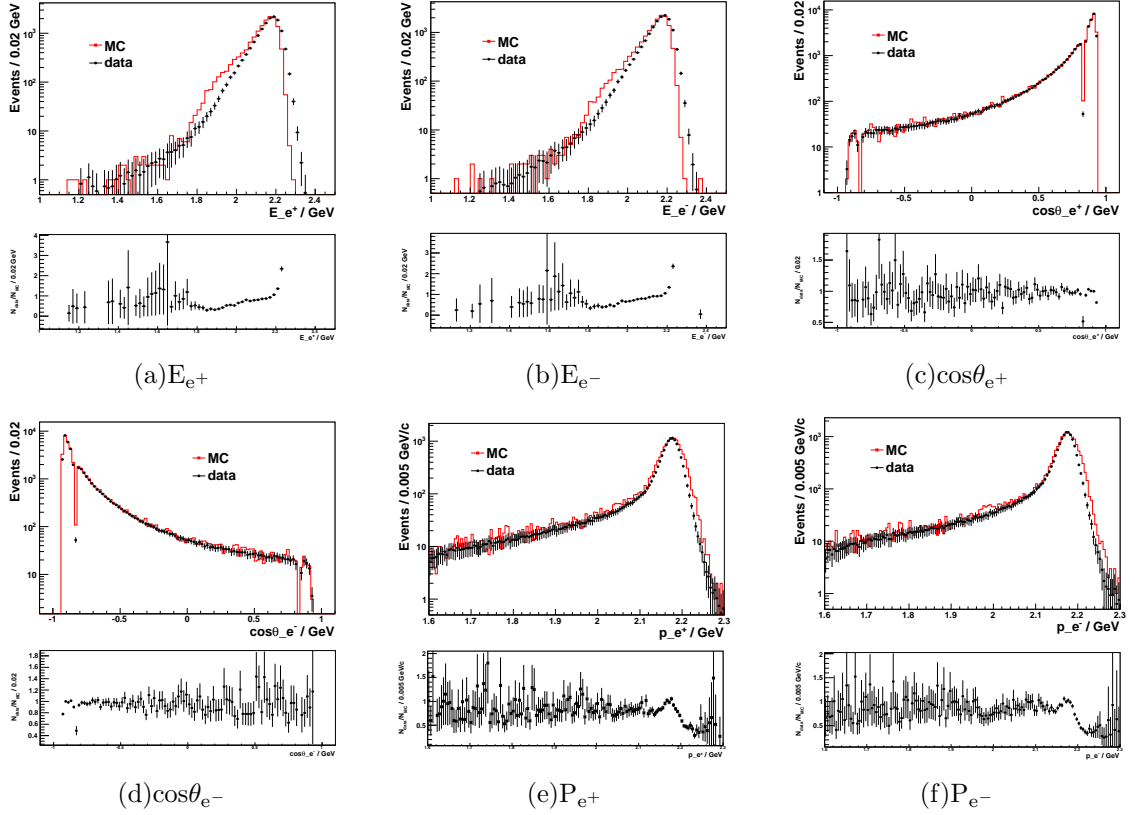


FIG. 21: The comparisons between data and MC in method I at 4360 MeV.

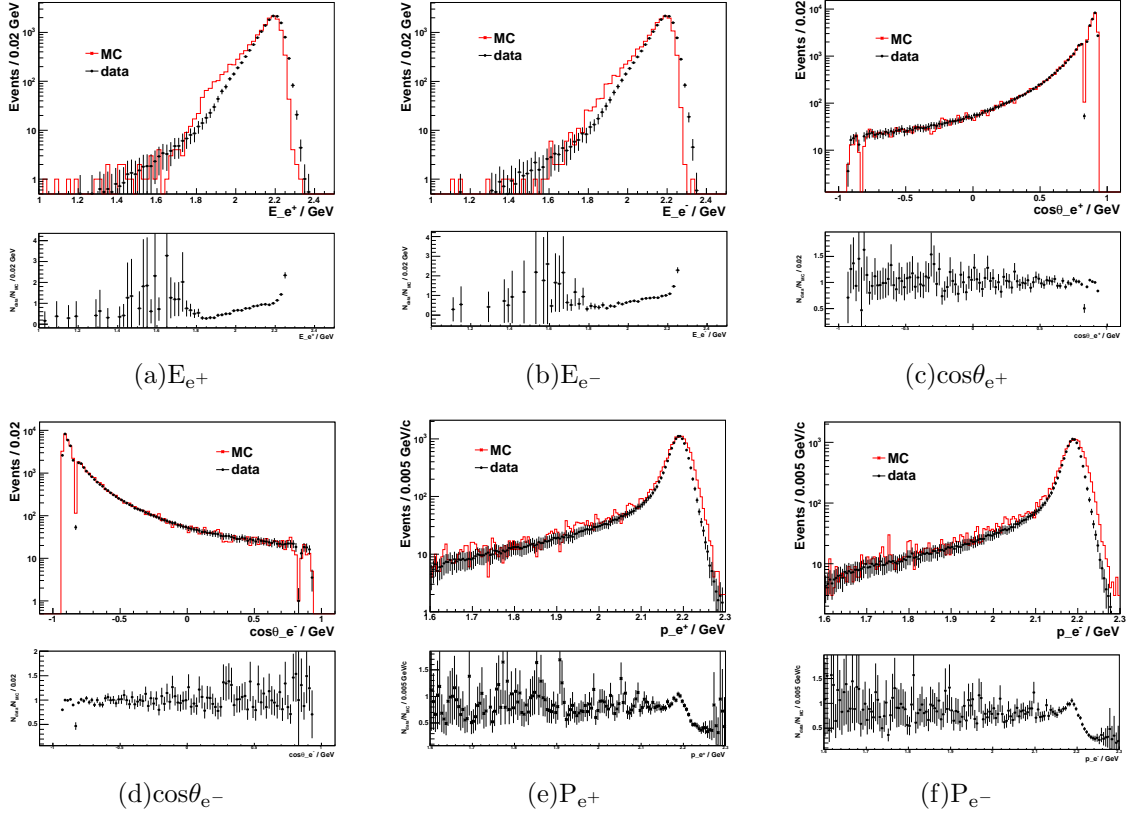


FIG. 22: The comparisons between data and MC in method I at 4390 MeV.

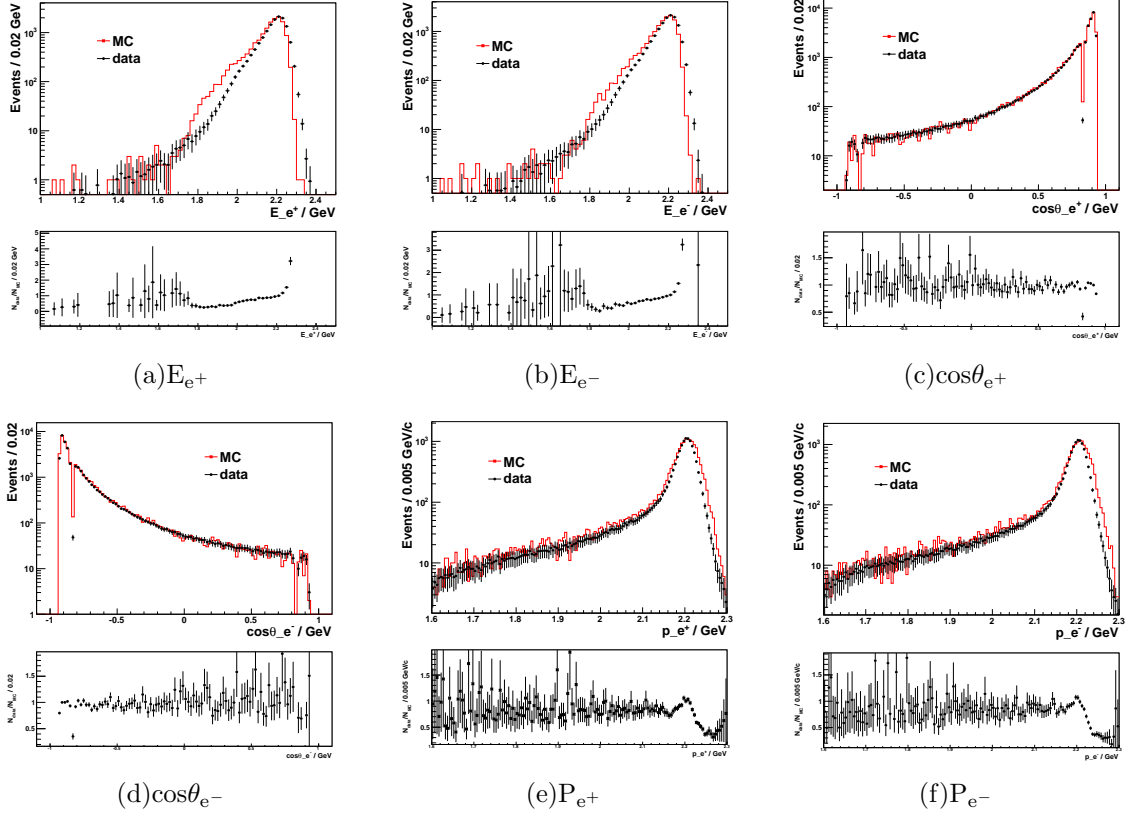


FIG. 23: The comparisons between data and MC in method I at 4420 MeV.

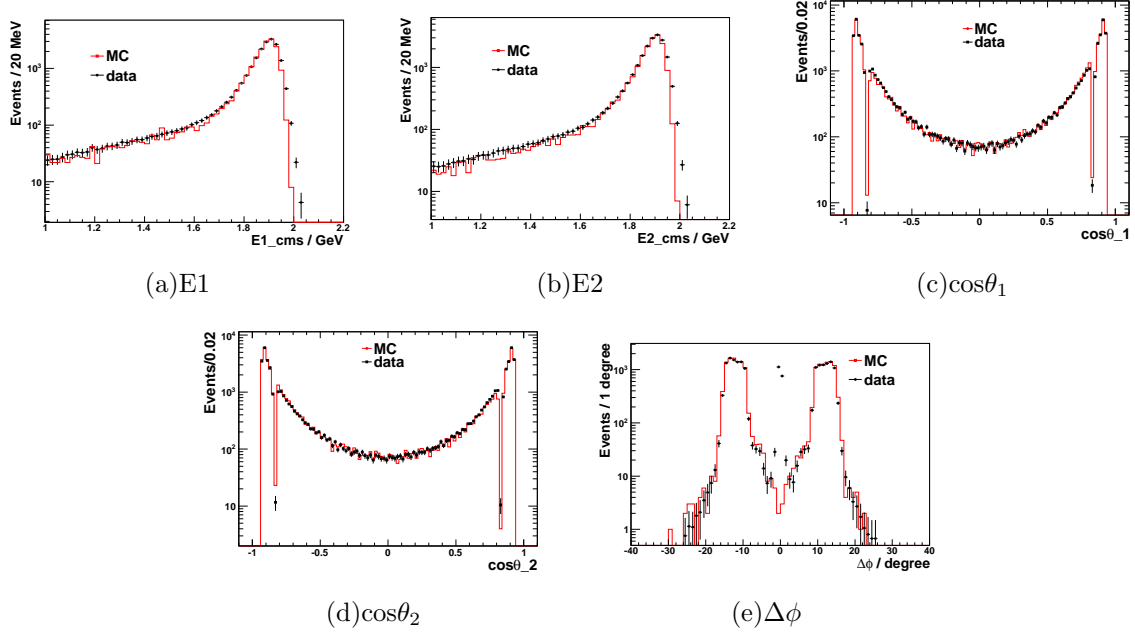


FIG. 24: The comparisons between data and MC in method II at 3810 MeV.

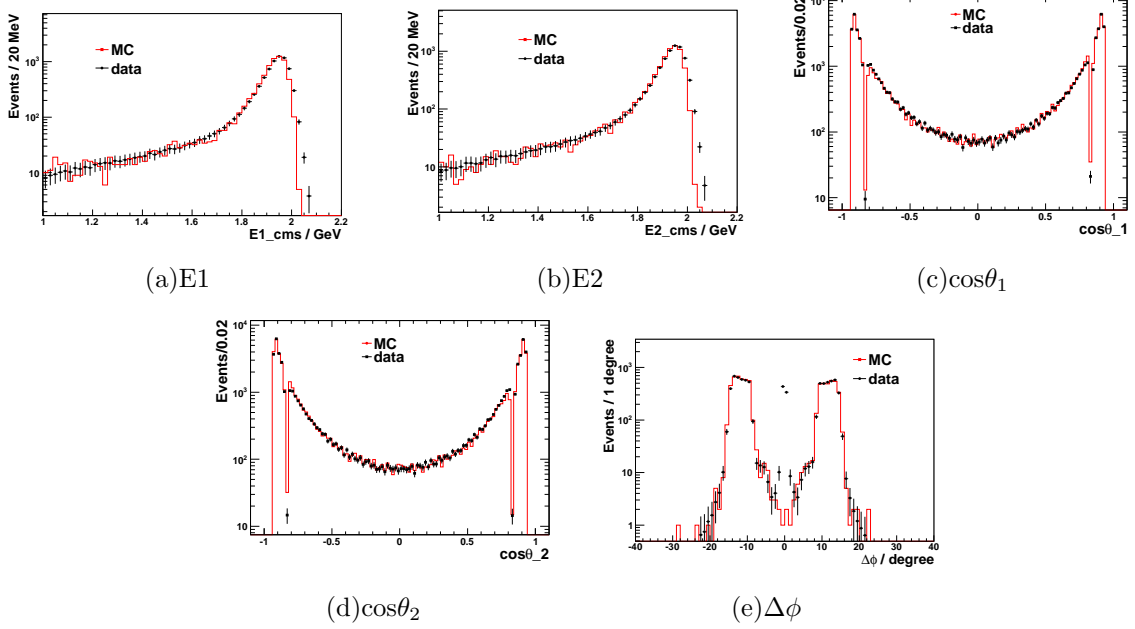


FIG. 25: The comparisons between data and MC in method II at 3900 MeV.

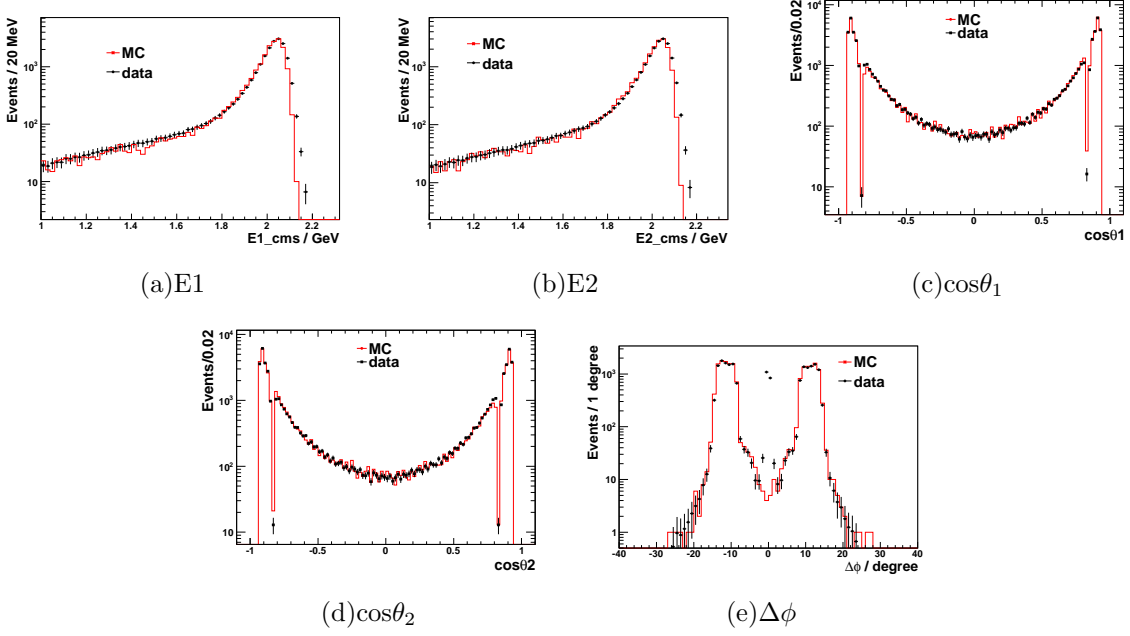


FIG. 26: The comparisons between data and MC in method II at 4090 MeV.

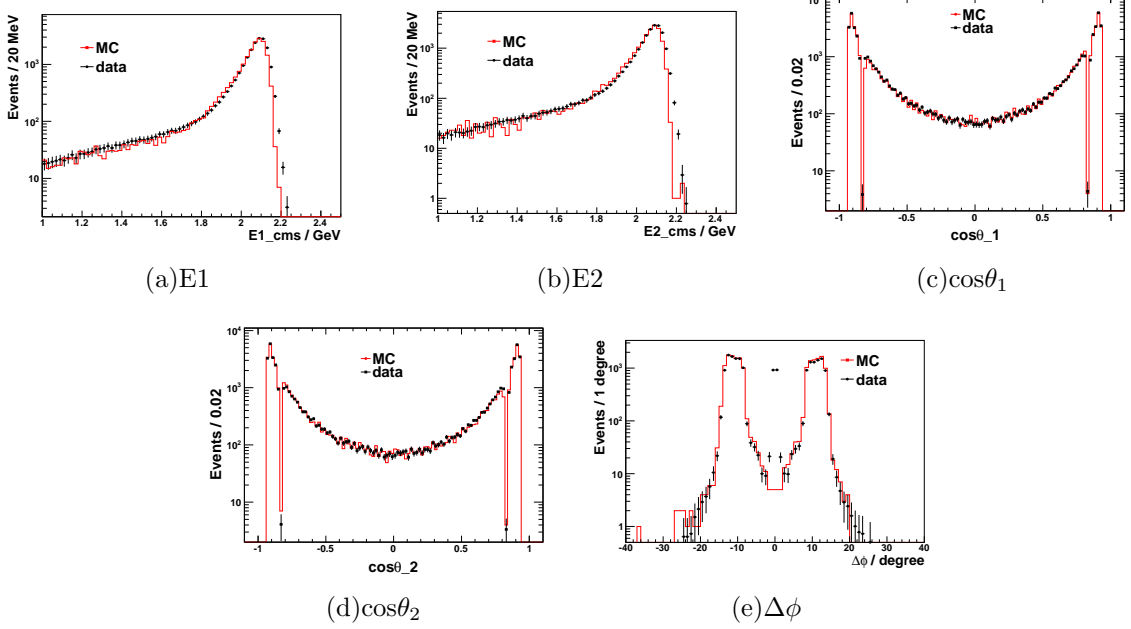


FIG. 27: The comparisons between data and MC in method II at 4190 MeV.

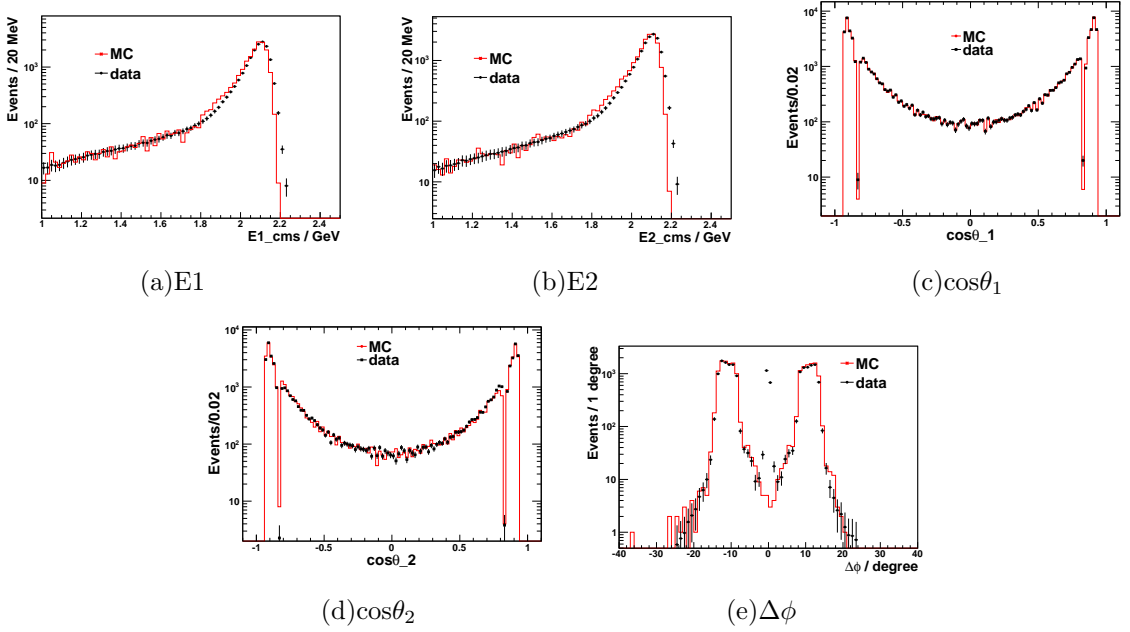


FIG. 28: The comparisons between data and MC in method II at 4210 MeV.

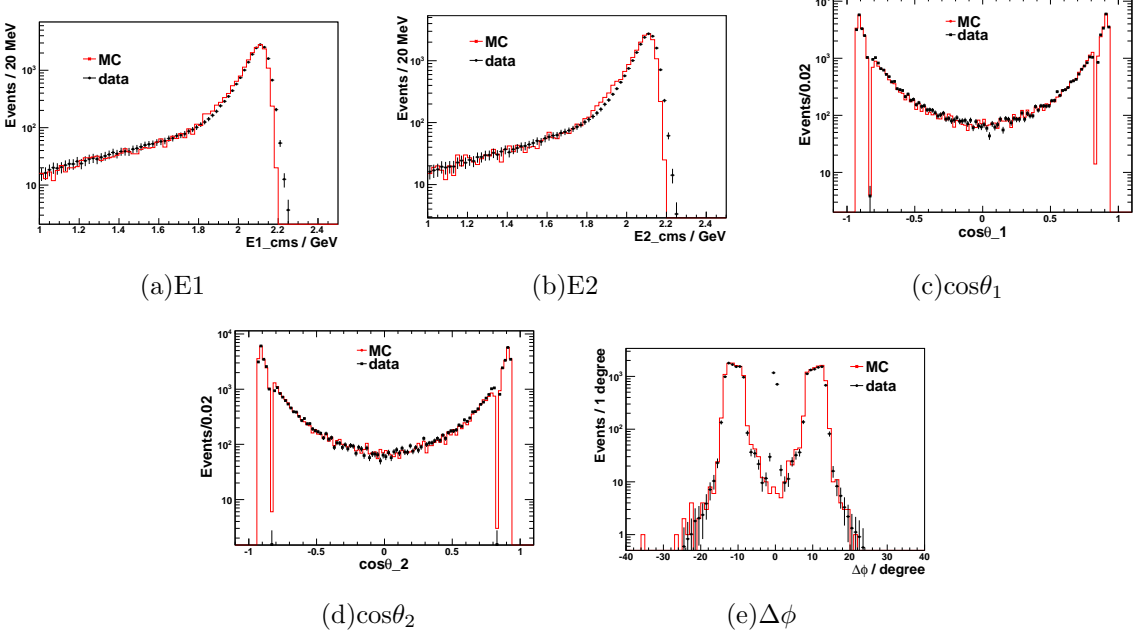


FIG. 29: The comparisons between data and MC in method II at 4220 MeV.

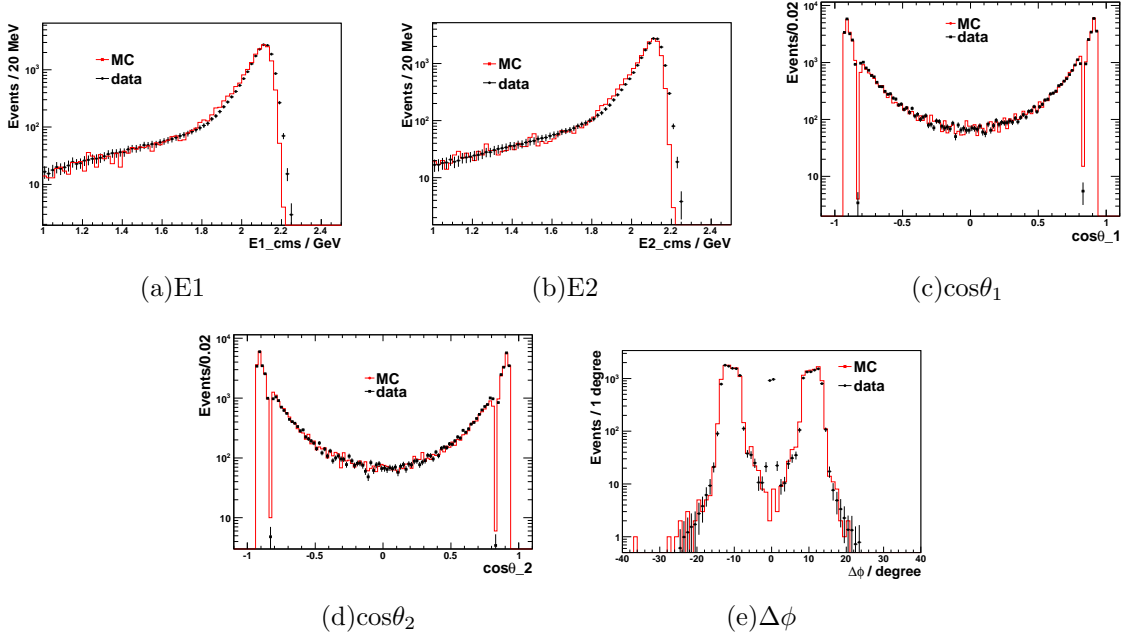


FIG. 30: The comparisons between data and MC in method II at  $4230^1$  MeV.

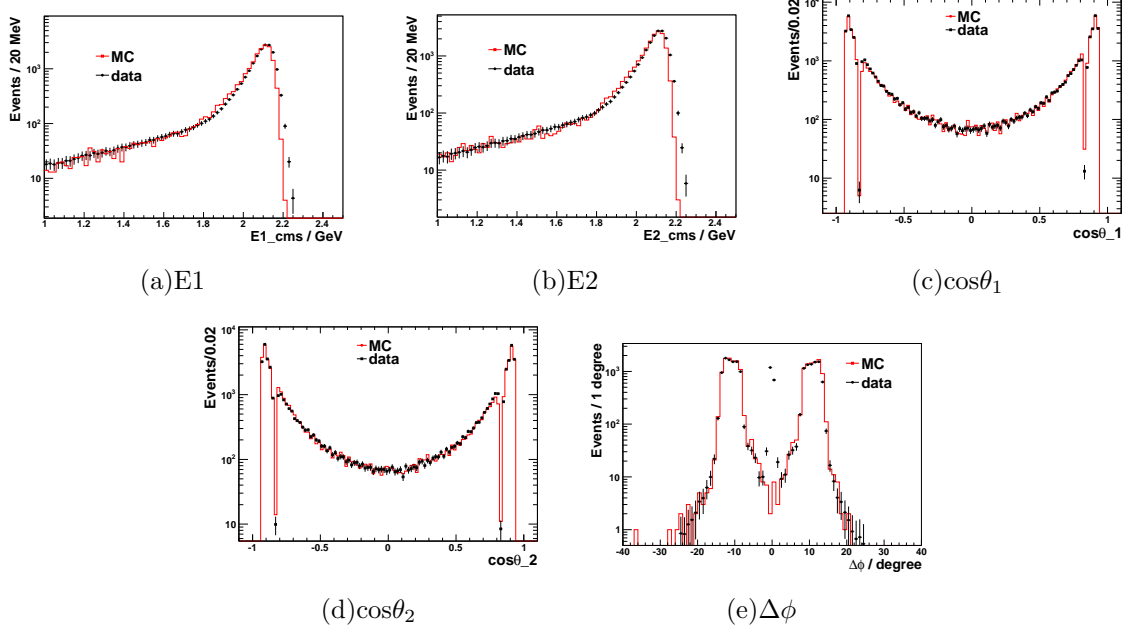


FIG. 31: The comparisons between data and MC in method II at  $4230^2$  MeV.

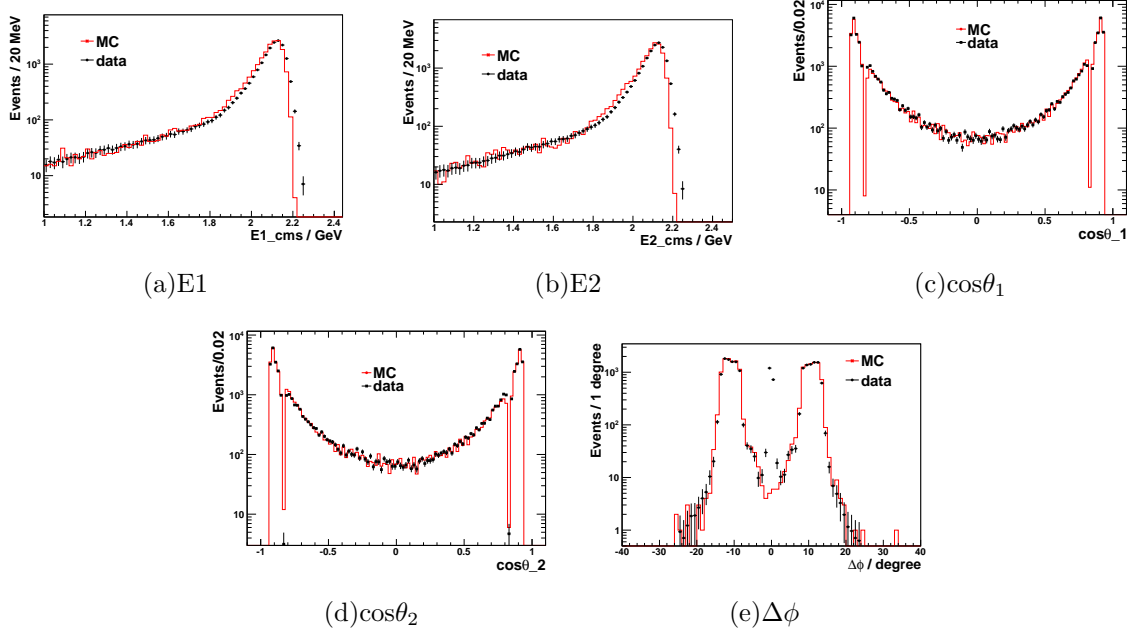


FIG. 32: The comparisons between data and MC in method II at 4245 MeV.

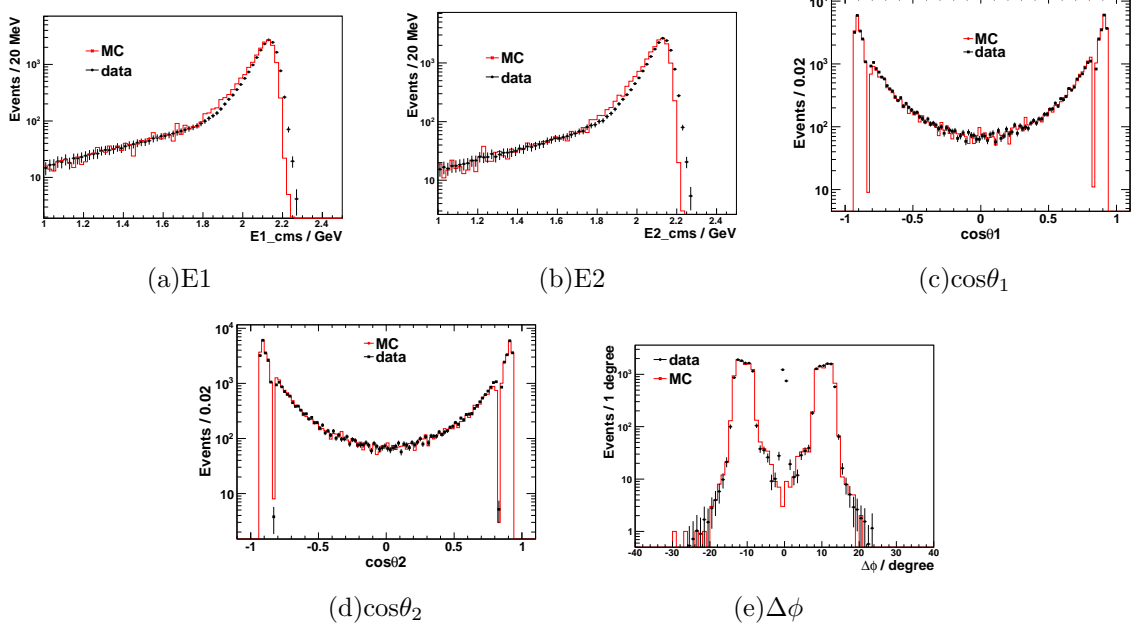


FIG. 33: The comparisons between data and MC in method II at 4260 MeV.

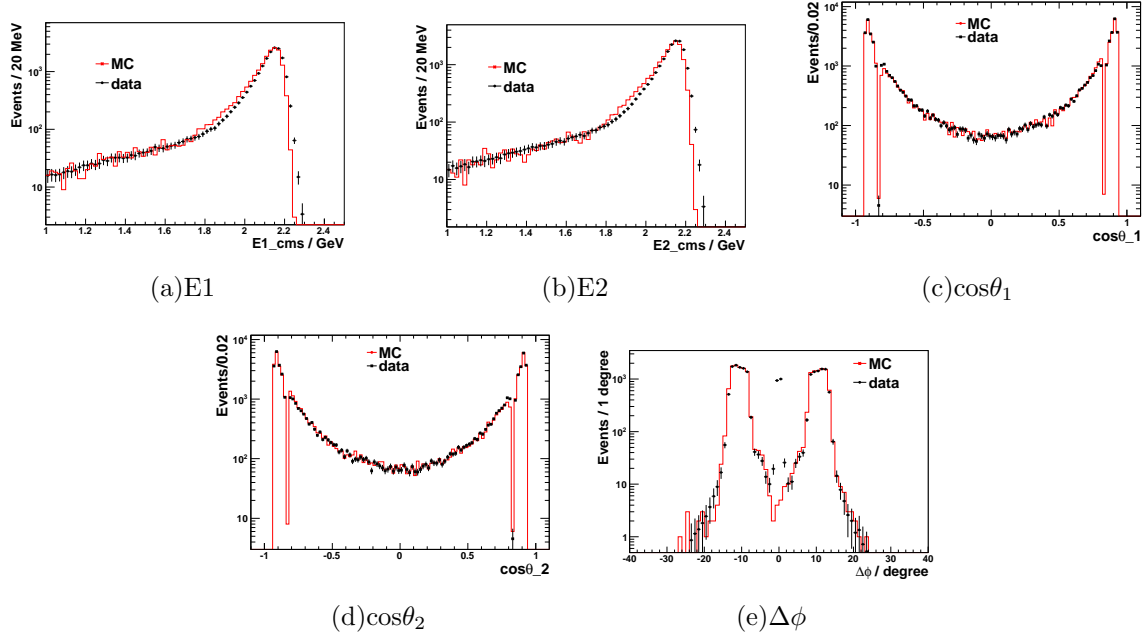


FIG. 34: The comparisons between data and MC in method II at 4310 MeV.

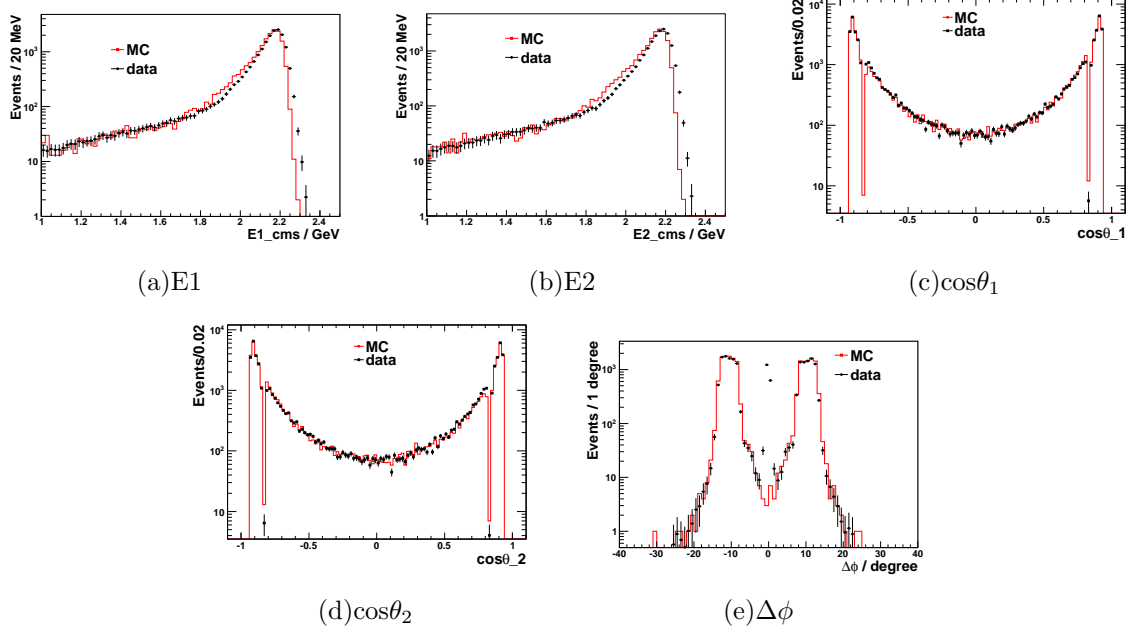


FIG. 35: The comparisons between data and MC in method II at 4360 MeV.

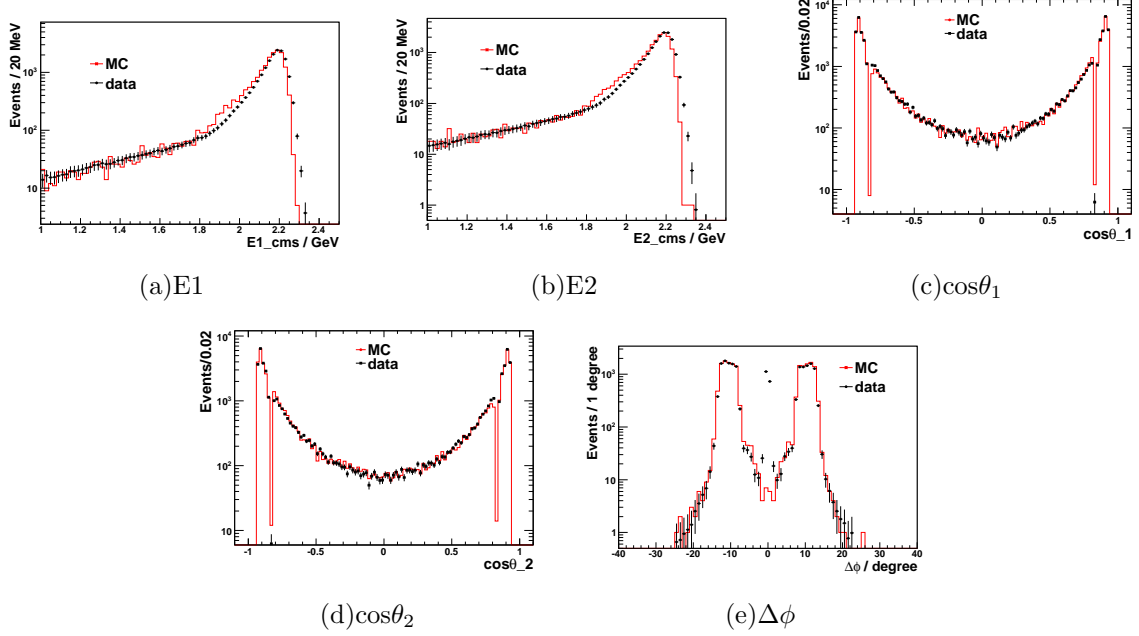


FIG. 36: The comparisons between data and MC in method II at 4390 MeV.

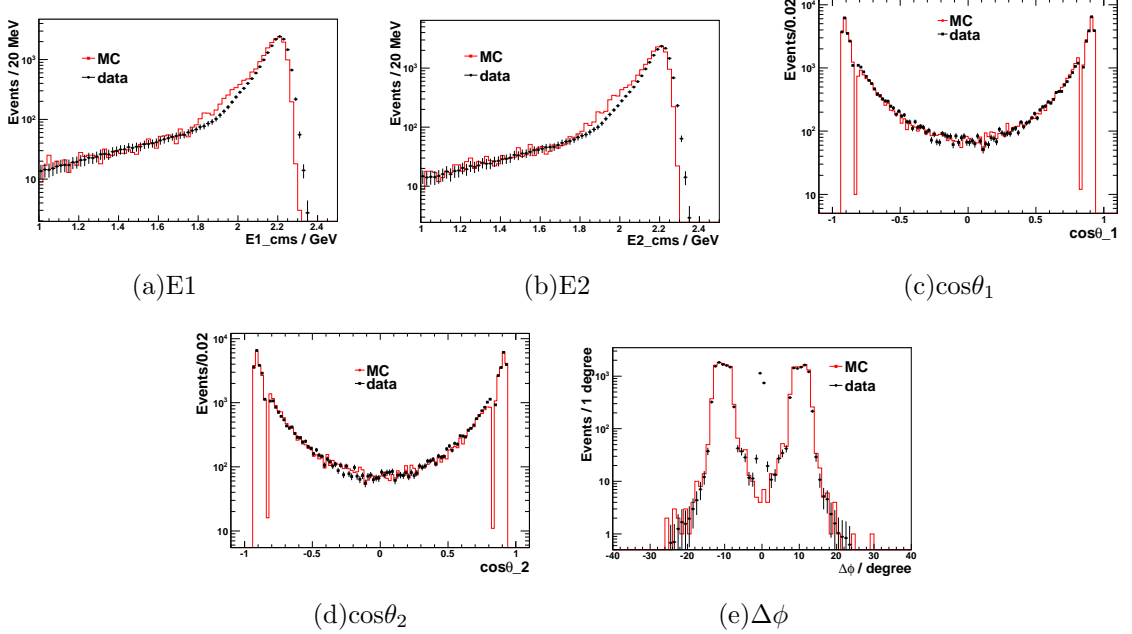


FIG. 37: The comparisons between data and MC in method II at 4420 MeV.

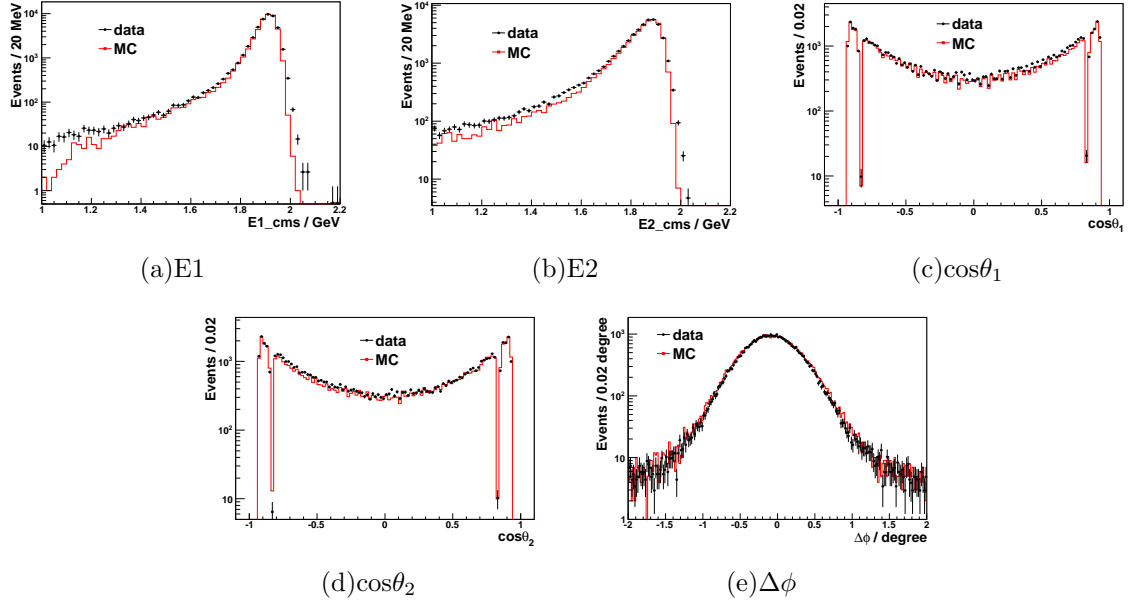


FIG. 38: The comparisons between data and MC in Digamma process at 3810 MeV.

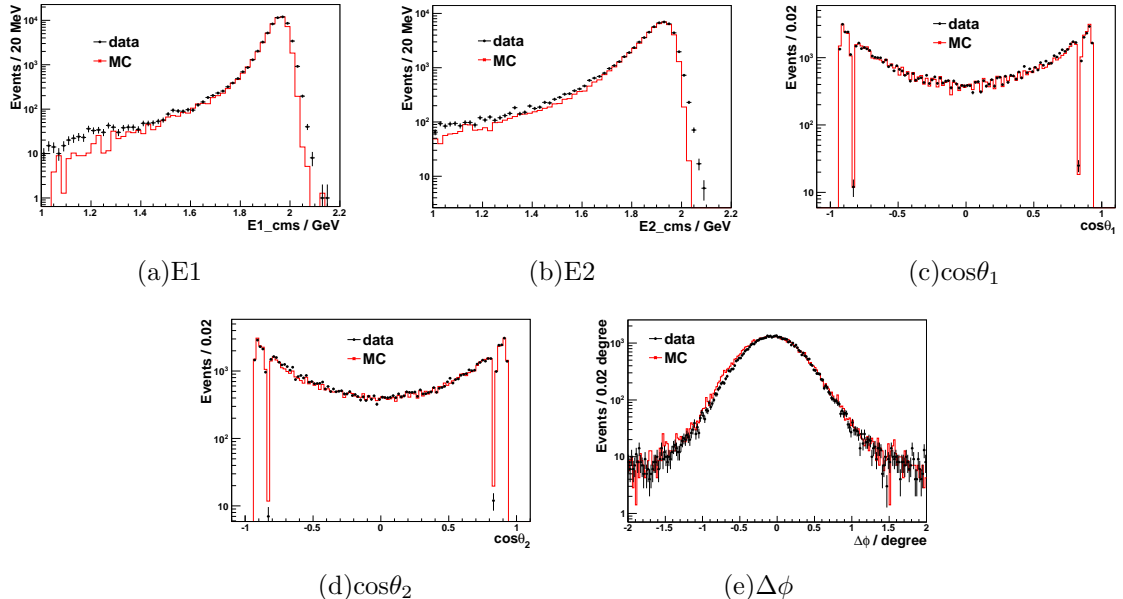


FIG. 39: The comparisons between data and MC in Digamma process at 3900 MeV.

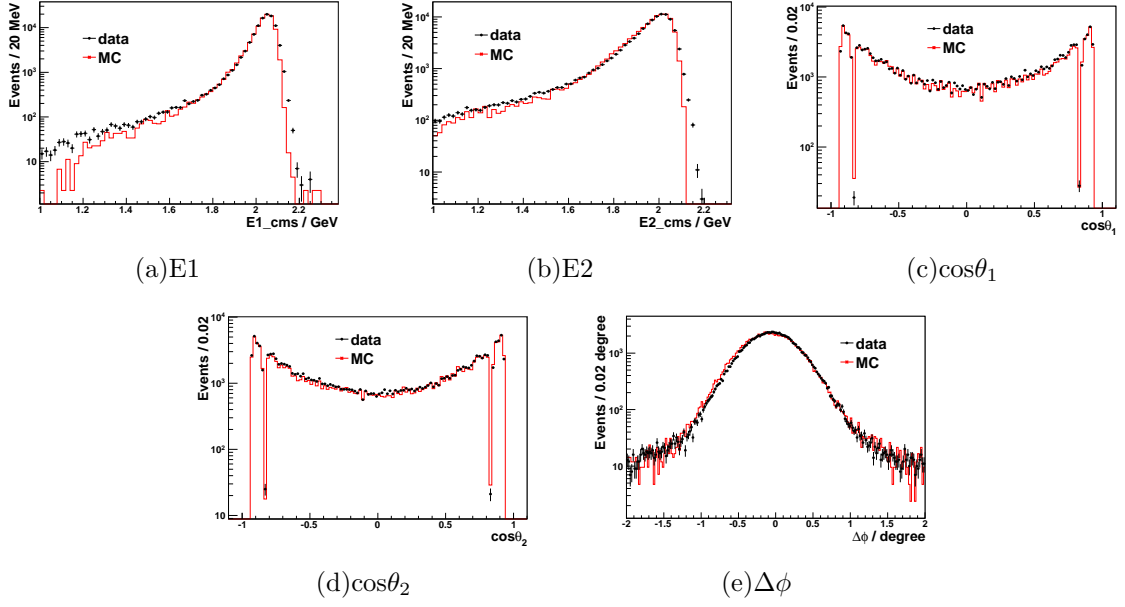


FIG. 40: The comparisons between data and MC in Digamma process at 4090 MeV.

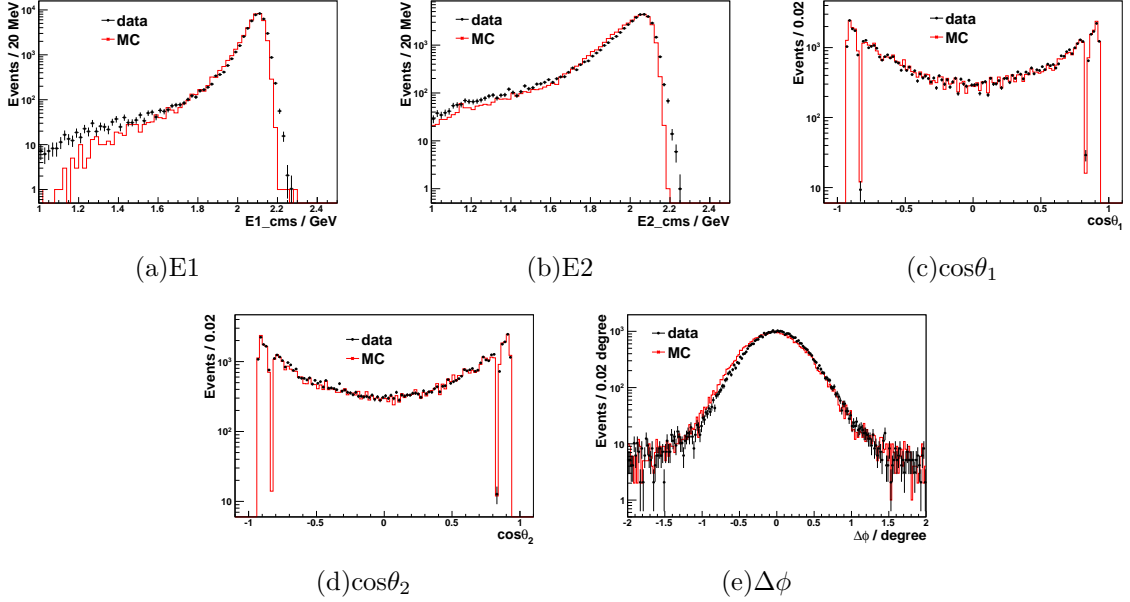


FIG. 41: The comparisons between data and MC in Digamma process at 4190 MeV.

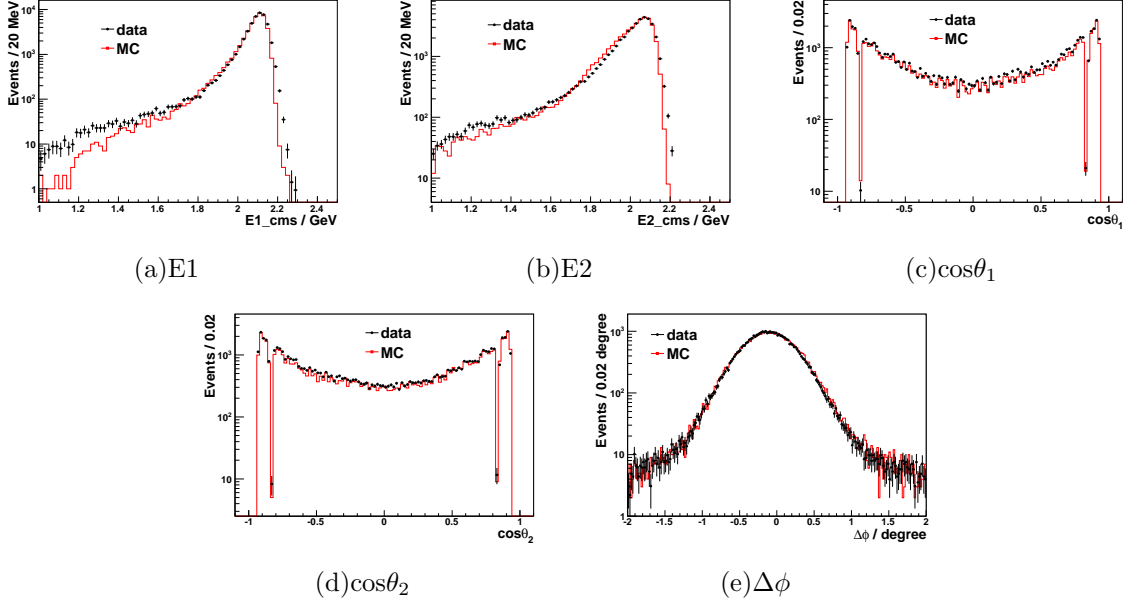


FIG. 42: The comparisons between data and MC in Digamma process at 4210 MeV.

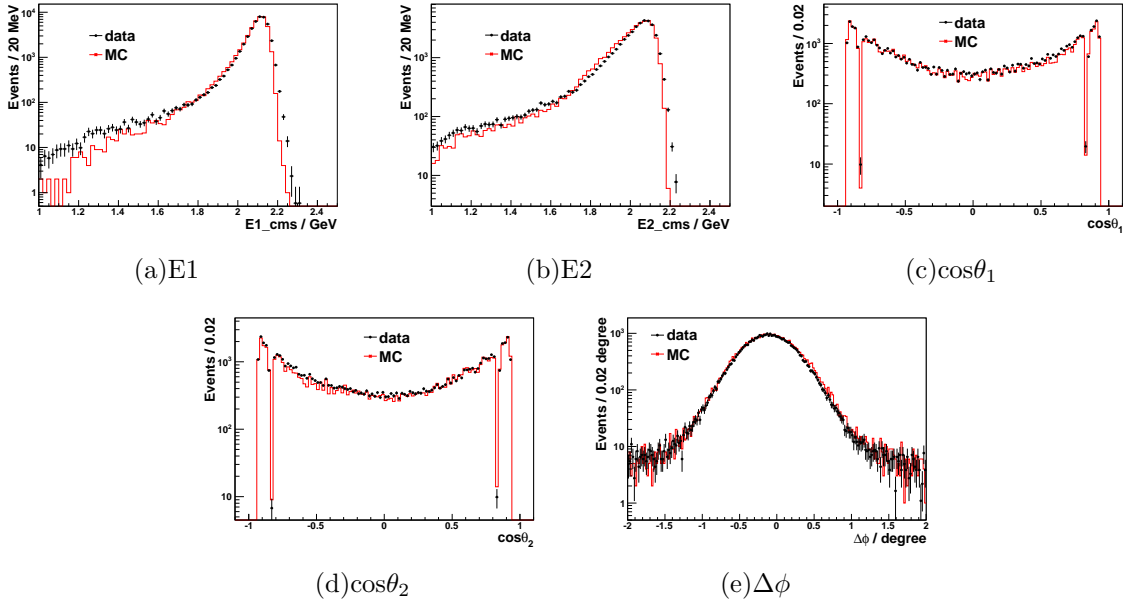


FIG. 43: The comparisons between data and MC in Digamma process at 4220 MeV.

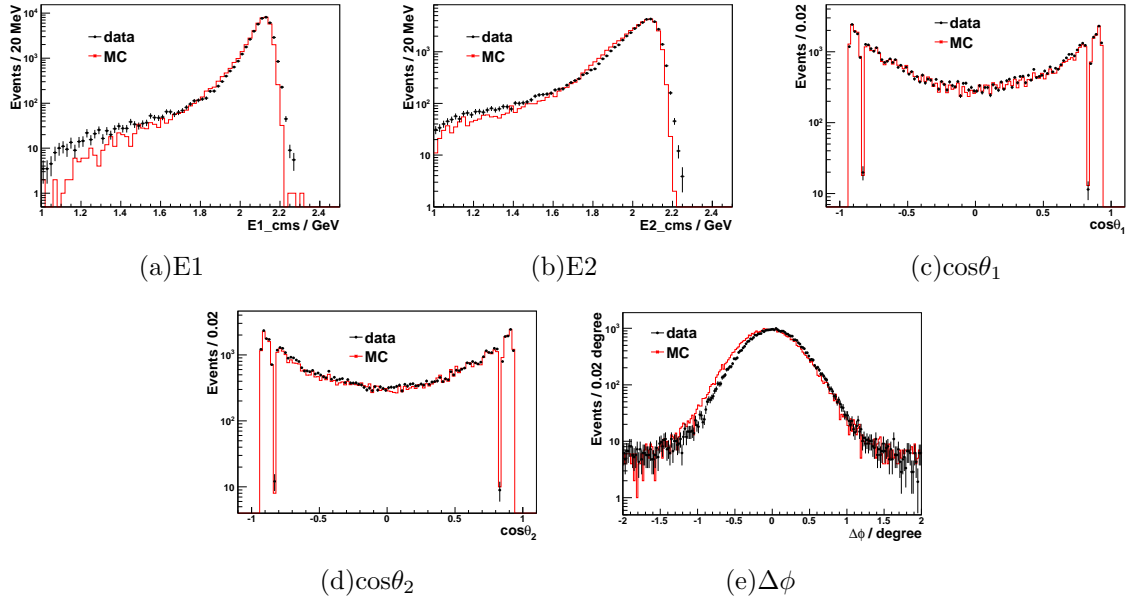


FIG. 44: The comparisons between data and MC in Digamma process at  $4230^1$  MeV.

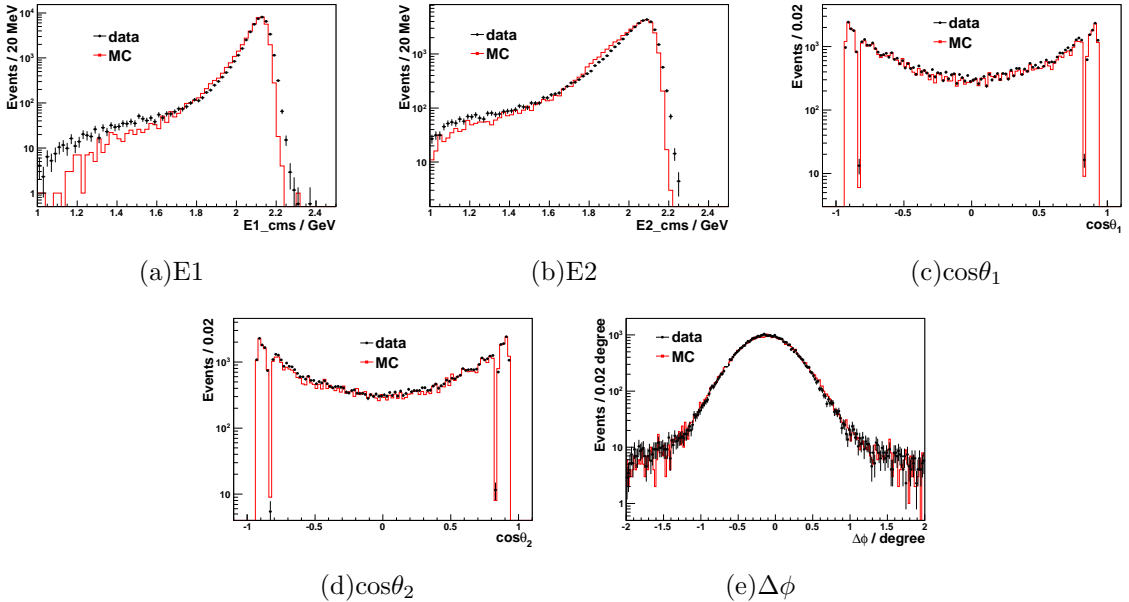


FIG. 45: The comparisons between data and MC in Digamma process at  $4230^2$  MeV.

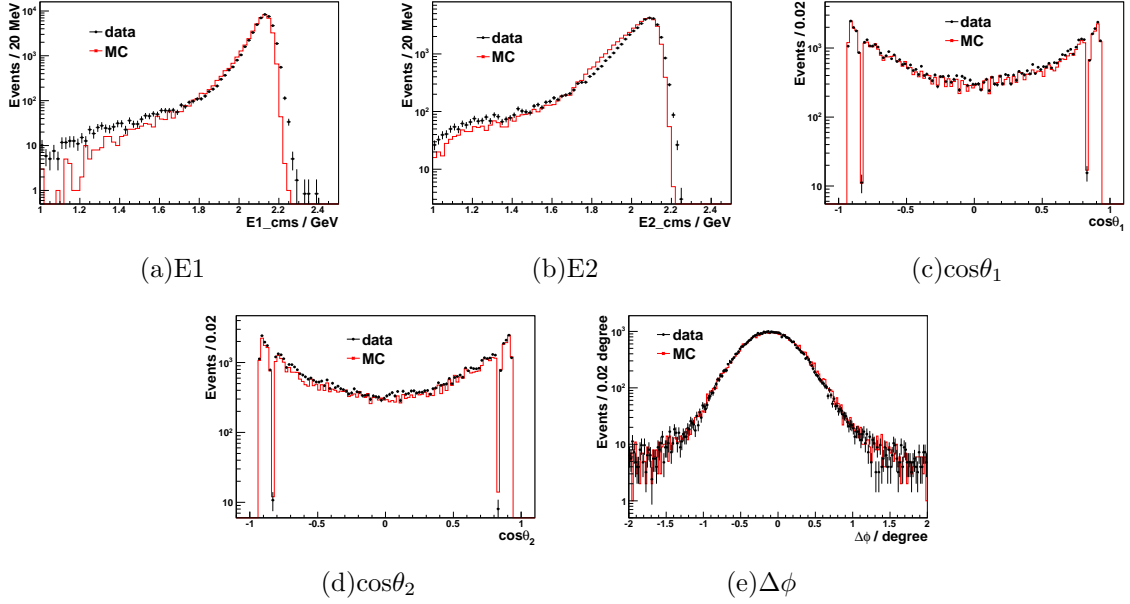


FIG. 46: The comparisons between data and MC in Digamma process at 4245 MeV.

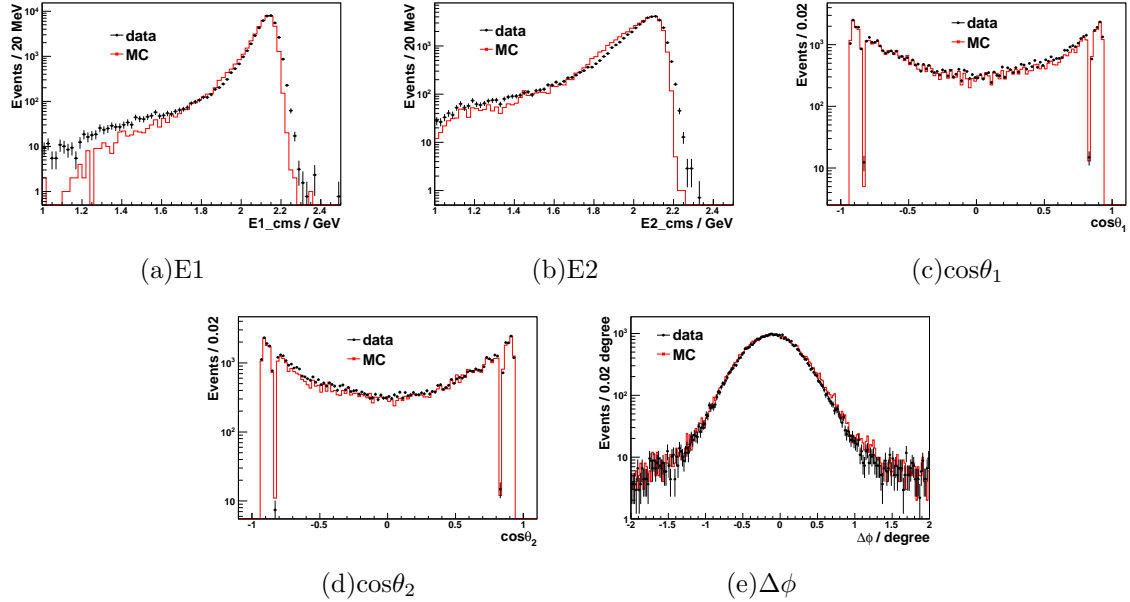


FIG. 47: The comparisons between data and MC in Digamma process at 4260 MeV.

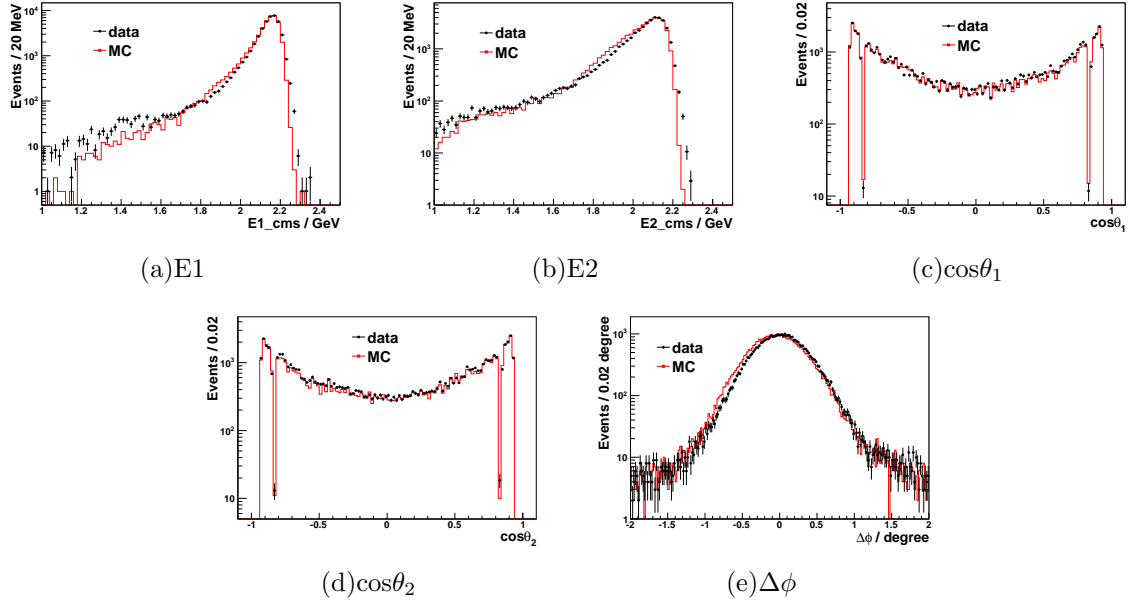


FIG. 48: The comparisons between data and MC in Digamma process at 4310 MeV.

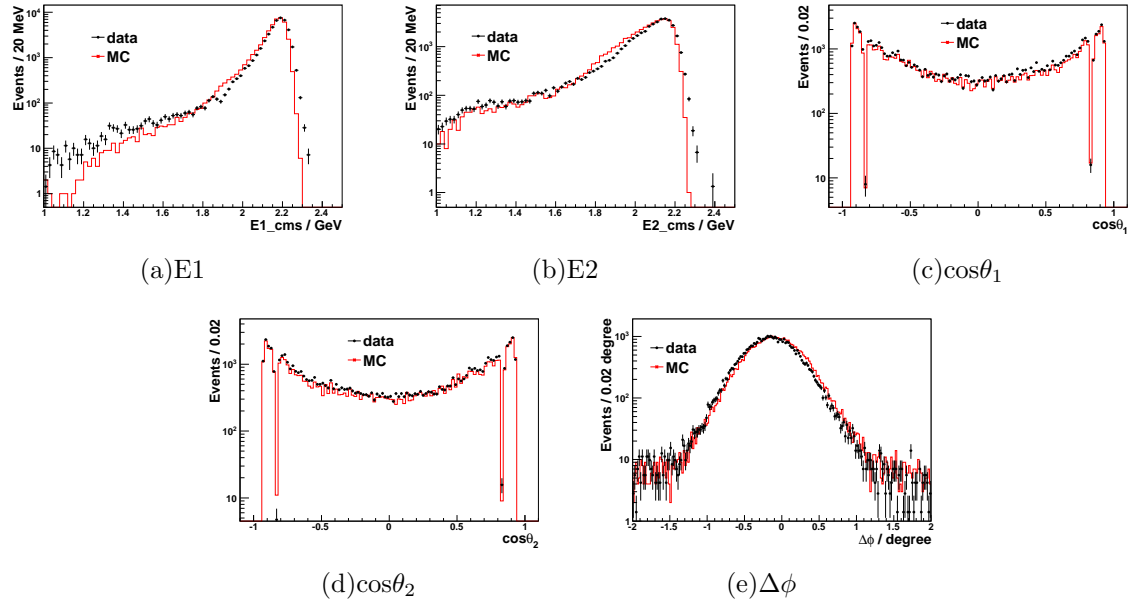


FIG. 49: The comparisons between data and MC in Digamma process at 4360 MeV.

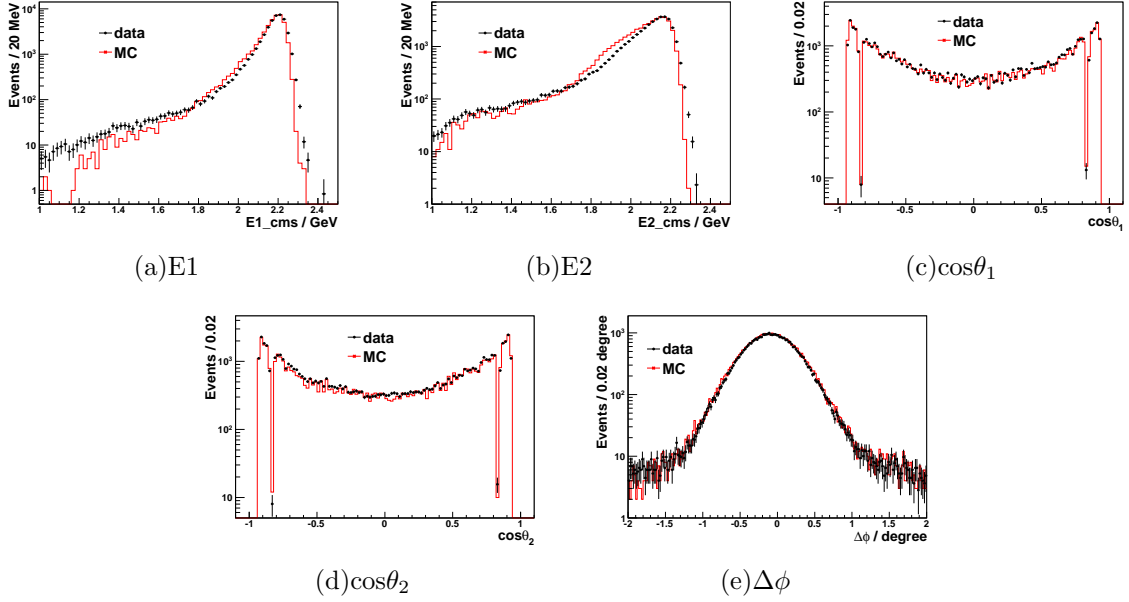


FIG. 50: The comparisons between data and MC in Digamma process at 4390 MeV.

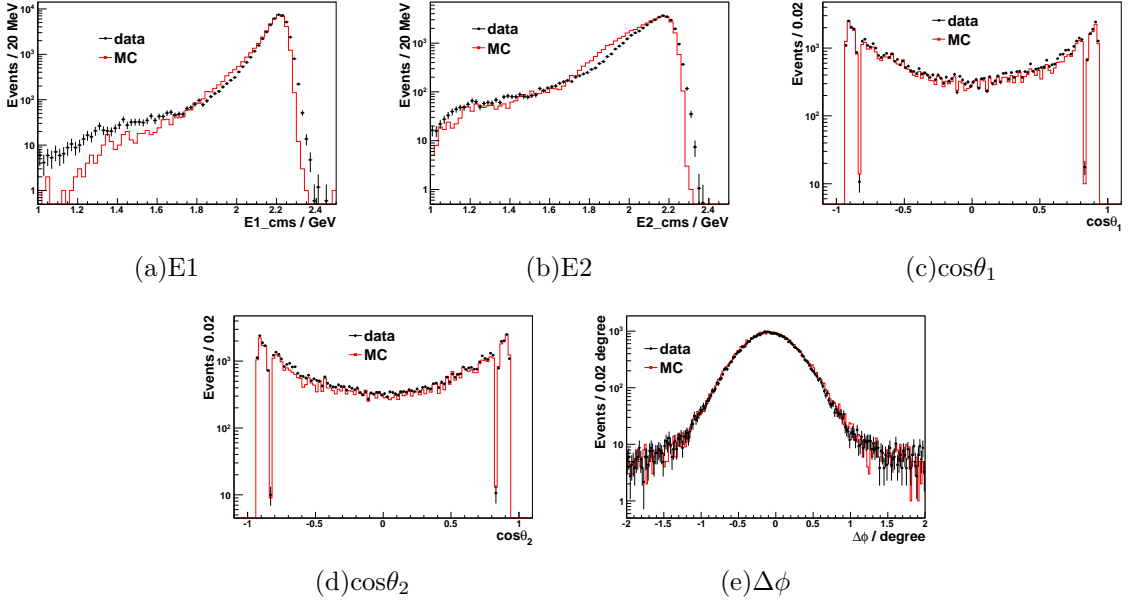


FIG. 51: The comparisons between data and MC in Digamma process at 4420 MeV.

## 241 VII. SUMMARY

242 From Table XIV, the total systematic error is 0.77% (averaged) or 1.00% (maximum), to  
 243 be simple and conservative, taking a systematic error of 1% (we recommend this value to  
 244 physics analysis using these data samples), we can get the luminosity results of all energy

245 points, as shown in Table XV and Figure 52. The results from Method I are consistent with  
246 those from the Di-gamma process, and the ones from Method I are taken as nominal results.

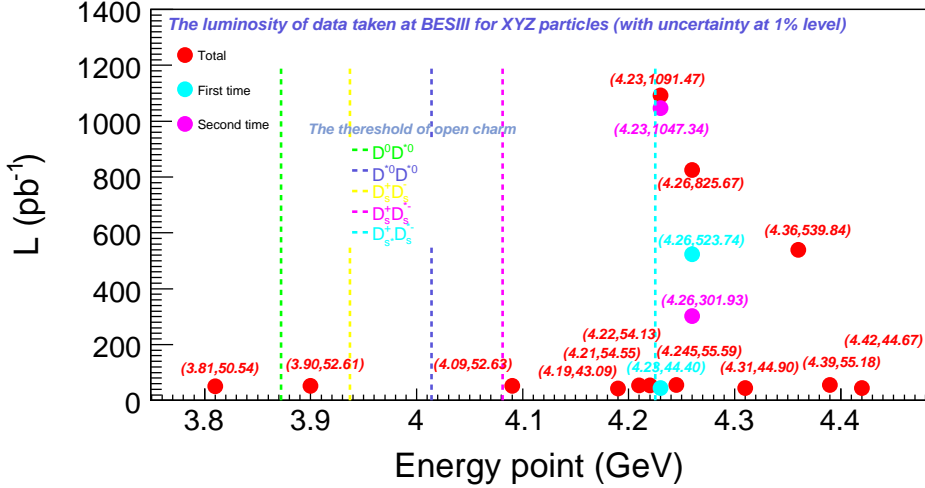


FIG. 52: The final result.

TABLE XV: Summary of the luminosity of all energy points with statistical and systematic errors, and 1% systematic errors are quoted here. The luminosity measured with Di-gamma process are also shown, where the errors are statistical only.

Num.	Energy(MeV)	Method I( $\text{pb}^{-1}$ )	Di-gamma( $\text{pb}^{-1}$ )
14	3810	$50.54 \pm 0.03 \pm 0.51$	$50.11 \pm 0.08$
15	3900	$52.61 \pm 0.03 \pm 0.53$	$52.57 \pm 0.08$
16	4090	$52.63 \pm 0.03 \pm 0.53$	$52.37 \pm 0.08$
3	4190	$43.09 \pm 0.03 \pm 0.44$	$43.08 \pm 0.08$
10	4210	$54.55 \pm 0.03 \pm 0.55$	$54.27 \pm 0.09$
11	4220	$54.13 \pm 0.03 \pm 0.55$	$54.22 \pm 0.09$
4	4230 <sup>1</sup>	$44.40 \pm 0.03 \pm 0.45$	$44.64 \pm 0.08$
13	4230 <sup>2</sup>	$1047.34 \pm 0.14 \pm 10.47$	$1041.56 \pm 0.37$
Tot	4230	$1091.74 \pm 0.15 \pm 10.92$	$1086.20 \pm 0.38$
12	4245	$55.59 \pm 0.04 \pm 0.56$	$55.52 \pm 0.09$
2	4260 <sup>1</sup>	$523.74 \pm 0.10 \pm 5.24$	$524.57 \pm 0.26$
9	4260 <sup>2</sup>	$301.93 \pm 0.08 \pm 3.02$	$301.11 \pm 0.20$
Tot	4260	$825.67 \pm 0.13 \pm 8.26$	$825.68 \pm 0.30$
5	4310	$44.90 \pm 0.03 \pm 0.45$	$45.46 \pm 0.08$
6	4360	$539.84 \pm 0.10 \pm 5.40$	$544.54 \pm 0.28$
7	4390	$55.18 \pm 0.04 \pm 0.55$	$55.89 \pm 0.09$
8	4420	$44.67 \pm 0.03 \pm 0.45$	$45.36 \pm 0.08$

- 
- 247 [1] S. Actis et al., Quest for precision in hadronic cross sections at low energy: Monte Carlo tools vs.  
248 experimental data Eur. Phys. J. C **66**, 585 (2010).
- 249 [2] W. M. Song *et al.*, Integrated Luminosity Measurement of Data Taken at 4.26 GeV, BESIII  
250 document 179-v1.
- 251 [3] W. M. Song *et al.*, Integrated Luminosity Measurement of Data Taken at 4.009 GeV, BESIII  
252 document 180-v1.
- 253 [4] Trigger efficiencies at BES-III, N. Berger, Zhu Kai et al. Chinese Physics C 34(12) (2010) 1779-  
254 1784.